

FACILITY FORM 802

N 65-36554  
(ACCESSION NUMBER)

49  
(PAGES)

CP 67554  
(NASA CR OR TMX OR AD NUMBER)

(TITLE)

1

(CODE)

13  
(CATEGORY)

GPO PRICE \$ \_\_\_\_\_

CSFTI PRICE(S) \$ \_\_\_\_\_

Hard copy (HC) 2.00

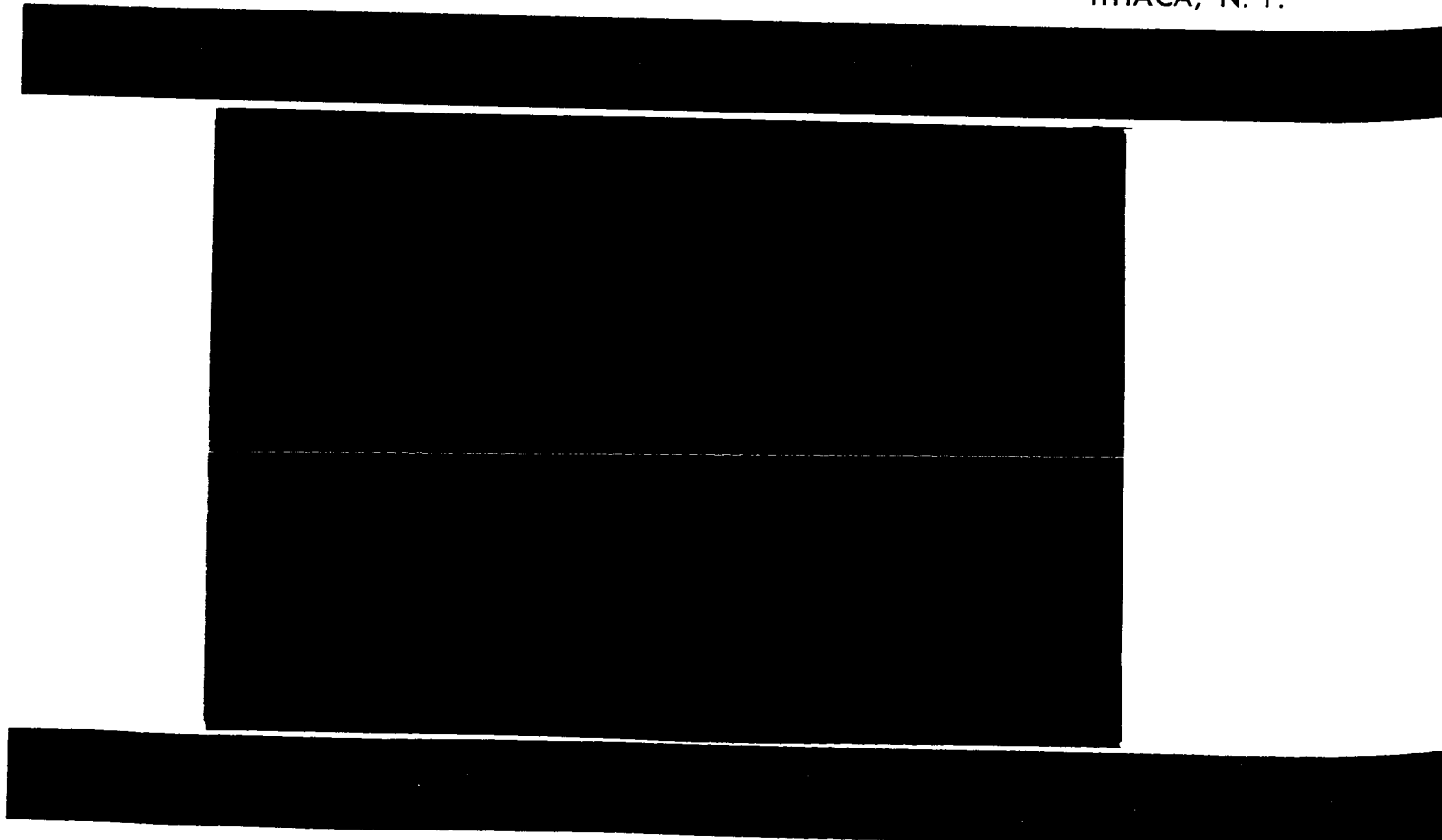
Microfiche (MF) 53

ff 653 July 65

# CORNELL UNIVERSITY

*Center for Radiophysics and Space Research*

ITHACA, N. Y.



CENTER FOR RADIOPHYSICS AND SPACE RESEARCH  
CORNELL UNIVERSITY  
ITHACA, NEW YORK

June 1965

CRSR 200

EFFECTS OF SEVERAL PARAMETERS ON THE OPTICAL  
PROPERTIES OF SOME ROCK POWDERS,  
WITH APPLICATIONS TO THE MOON

Hsiu Yung Chen Chow

## ACKNOWLEDGMENTS

The work reported here was performed under the direction of Dr. B. Hapke, I am deeply indebted to him for his patient advice and inspiration during the course of my research, without which this work could not have been done. I also wish to thank R. Pipher and G. Strasser for their help.

This work was supported by the National Aeronautics and Space Administration under NASA Grant Nsg-382.

## I. INTRODUCTION

The nature of the lunar surface is one of the currently interesting problems in astrophysics. From observations of the thermal, radar and optical properties of the lunar surface, it has been generally concluded that the moon's surface is covered with a layer of fine powder.<sup>(1,2)</sup>

The light-reflecting properties of the lunar surface appears to be an important source of our knowledge of its microscopic structure. The primary goal of this experiment is to investigate the effect of several parameters on the optical properties of some rock powders; this will further reduce the range of materials which may be thought of as composing the moon's surface.

The optical properties investigated were:

1. Relative brightness as a function of angle of incidence and observation,
2. Linear polarization dependence on these angles,
3. Normal albedo as a function of color,
4. In addition, a limited investigation of the dependence of brightness and polarization on wavelength at a few selected angles was undertaken.

The parameters of the surface investigated were:

1. Particle size,

2. Surface compaction,
3. Effects of irradiation by  $\gamma$ -ray, 2 kev hydrogen ions and 2 kev helium ions.
4. Dose of hydrogen ion irradiation,
5. Composition.

The following definitions and notations will be used in this paper:

Normal albedo:  $B$  --- the ratio of brightness of a surface to that of a perfectly diffusing white surface, both surfaces viewed and illuminated normally.

Polarization:  $P = \frac{I_+ - I_-}{I_+ + I_-}$ , where  $I_+$  and  $I_-$  are the intensity of light with vibrations perpendicular and parallel respectively to the plane determined by the directions of illumination and observation.

Phase angle:  $\phi$  --- angle between directions of illumination and observation.

Inversion angle:  $\phi_0$  --- phase angle (other than at  $\phi = 0^\circ$ ) at which the polarization of light reflected from a surface is zero.

$B_R$ ,  $B_G$  and  $B_B$  --- normal albedo of the surface in red, green and blue light respectively.

Angle of incidence:  $i$  --- angle which the direction of the incident ray makes with the normal to the surface.

Angle of observations:  $\epsilon$  --- angle which the reflected ray makes with the normal to the surface.

## II. PHOTOMETRIC PROPERTIES OF THE MOON

The optical properties of lunar surface, as summarized by B. Hapke<sup>(3)</sup> are characterized by several unusual features: (typical curves are illustrated in fig.1.)

- "1. The albedo is uniformly low, varying from about 5% to 18%.
2. The surface strongly backscatters light so that the intensity of the sunlight reflected toward the earth from nearly all areas on the moon reaches a sharp maximum at full moon.
3. The polarization is zero at full moon, but becomes negative for small phase angles, reaching a minimum of 1.2% at a phase angle of  $11^{\circ}$ ; at about  $23^{\circ}$  the plane of polarization suddenly rotates, the polarization going through zero and becoming positive, and reaching a broad maximum near  $110^{\circ}$  phase. The maximum polarization is uniformly small, seldom exceeding 15%. Brighter formations on the moon generally polarize the light less strongly. No elliptical polarization has been detected.
4. The manner in which both the polarization and brightness of a region vary during a lunation is almost exclusively a function of the lunar phase angle, and

is very nearly independent of location on the lunar sphere and of the type of terrain."

5. Even though the moon is essentially colorless, moonlight exhibits some dependence on wavelength. The normal albedo varies directly with wavelength, while the positive polarization peak varies inversely with the wavelength. If  $B_G$  is normalized to  $B_G = 10$ , the ratio of  $B_R/B_G$  and  $B_B/B_G$  is between 12.0 --- 13.2 and 6.3 --- 7.6, respectively. For brighter regions  $B_B/B_G$  is lower than for darker regions<sup>(4)</sup>

A variety of terrestrial surfaces have been carefully studied photometrically by many authors (see references given in (2)), but their optical properties do not generally resemble those of the surface of the moon.

Hapke and Van Horn<sup>(2)</sup> suggested that the sharp backscatter properties of the moon could be duplicated by fine powders darkened by hydrogen ion bombardment to simulate the solar wind hitting the lunar surface. This suggestion was independently confirmed by B. Hapke<sup>(5)</sup> and G. K. Wehner and his coworkers<sup>(6)</sup>. B. Hapke<sup>(5)</sup> also studied the effect of simulated solar wind and found that hydrogen ion bombardment changes the albedo, color, polarization and light scattering properties of some selected rock powders; the change is invariably toward the lunar photometric characteristics.

One of the major components of the corpuscular radiation flux at the lunar surface is the solar wind, which consists of electrons and of ions of hydrogen, helium, and probably heavier atoms. The existence of the solar wind, which had long suspected, has now been verified by space vehicle experiments<sup>(7)</sup>. The solar wind particles are believed to be primarily of energy less than a few kev. The flux of protons in the solar wind in interplanetary space, as measured by Mariner II, is about  $2 \times 10^8$  protons/cm<sup>2</sup> sec. with 600 km/sec average velocity.



### III. EXPERIMENTAL APPARATUS AND PROCEDURE

Two major pieces of apparatus are used in this experiment: The ion gun, which produces the simulated solar wind, and the photometer, which measured the optical properties of various surfaces.

#### 1. Ion bombardment

The ion gun is part of an ultra-high vacuum chamber and is shown schematically in fig. 2. Hydrogen gas is ionized by electrons emitted from the upper filament to form a hydrogen plasma. The hydrogen ions passing through the grids are accelerated through a potential of 2 kilovolts toward the target, whereas the electrons are repelled back toward the plasma. A second tungsten filament is inserted across the beam in order to provide current-neutralization; this is necessary to prevent the potential on the surface of the insulator target from charging to a high positive value and repelling the ions.

Before irradiation, the sample was placed on the top of the sample stand and pumped down to a low pressure. During bombardment the partial pressure of hydrogen gas at the sample was about  $1 \times 10^{-4}$  torr (uncorrected ion gauge reads  $5 \times 10^{-5}$  torr). Partial pressure of other gases in the system is less than  $1 \times 10^{-8}$  torr; this is mostly water vapor, as determined by a residual gas analyzer. The

temperature of the sample during irradiation does not exceed  $170^{\circ}\text{C}$ . The beam is unanalyzed and contains some  $\text{H}_2^+$  and  $\text{H}_3^+$  ions as well as protons. The ion current density is about  $1 \text{ ma/cm}^2$ . At this current density, an irradiation of one day in the laboratory is equivalent to about  $2 \times 10^5$  years on the moon, assuming the flux at the lunar surface is the same as in interplanetary space.

The ion beam current is monitored by measuring the current between the neutralization filament and ground, since with an insulating target the ion current cannot be measured directly. Measurements with conducting targets show that this current is equal to the ion beam current to within 10%.

## 2. Photometer

The photometer consists of a light source mechanically chopped at 20 cps and an AC detector; thus the measurement need not take place in a completely dark room (see fig. 3). The power supply of the light source has intensity-regulated feedback to keep light output variations less than 0.1%. A system of lenses projects the light onto the surface being investigated to form a uniformly illuminated spot 3 inches diameter; but the detector observes an area only  $1/2$  inch in diameter. The distances from both source and detector to the test surface is 18 inches.

The intensity and polarization curves in this experiment were taken by varying the angle of incidence  $i$ , while

the angle of observation  $\epsilon$  was fixed at two angles:  $\epsilon = 0^\circ$  and  $\epsilon = 60^\circ$ . The directions of incidence and observation and the normal to the surface are coplanar. A certain spot on the moon as seen from the earth maintains the angle of observation approximately constant during the course of a month, while the angle of incidence varies. Curves taken at the two given angles of observation in the laboratory give sufficient information to decide whether the surface is similar to the moon. The amount and direction of polarization are measured by rotating the polaroid film. A special circuit is incorporated in the detector which cancels out most of the incoming signal and allows very small variations in the intensity to be measured. A Lyot<sup>(8)</sup> depolarizer is inserted in the light source to eliminate all polarization which might be produced by the source. The normal albedo is determined by measuring the brightness of the specimen at  $\epsilon = 0^\circ$  and  $i = 2^\circ$  relative to the brightness at the same angles of a standard surface of MgO powder. The latter surface closely approximates a Lambert surface and has an albedo of nearly unity over the visible portion of the spectrum.<sup>(9)</sup>

The red, green and blue interference filters used have effective wavelengths at  $6450\text{\AA}$ ,  $5600\text{\AA}$  and  $4240\text{\AA}$  respectively, with band widths of about  $500\text{\AA}$ . Without the filters the photometer responds to wavelengths between about  $4000\text{\AA}$  to  $7000\text{\AA}$  with a curve somewhat flatter than the response curve of the human eye. All the optical curves measured with the

angle of incidence varying as described above were taken in white light. The normal albedo and also the polarization and brightness at ( $\epsilon = 60^\circ$ ,  $i = -30^\circ$ ,  $\phi = 90^\circ$ ) were investigated at the wavelengths of red, green and blue filters. (A negative value of  $i$  means that  $i$  is on the opposite side of the normal to the surface from  $\epsilon$ .)

### 3. Error

The principal source of error of this experiment is noise due to thermionic emission from the photocathode. The error resulting from this effect was estimated by measuring the photometric properties of a surface several times. The error in intensity (standard deviation) is less than  $\pm 2\%$ . The error in polarization for a high-albedo surface ( $B = 30\%$ ) is around  $\pm 0.1\%$ , while for a low-albedo material ( $B = 5\%$ ) the error in polarization is raised to  $\pm 0.2\%$ . These are conservative estimates.

#### IV. RESULTS AND ANALYSIS

All rock powders after irradiation by H ions change their color and are reduced in albedo. The darkening effect is striking and is not a result of deposition of cracked pump oil or other spurious effects, because many solid objects exposed to the beam do not darken at all, and materials like MgO, Al<sub>2</sub>O<sub>3</sub> and SiO<sub>2</sub> powders either do not darken or darken only slightly.

The major darkening mechanism, as postulated by B. Hapke<sup>(5)</sup>, is due to differential collection of sputtered material. Atoms sputtered from a smooth surface completely leave the surface, but from a rough surface with overhangs, the sputtered atoms are caught on the undersides of the structures composing the surface. Oxygen, being a volatile element, probably has a lower sticking probability than metals or silicon; hence the collected sputtered material may be deficient in oxygen and richer in Si and metals than the parent mineral. Such a non-stoichiometric coating on the bottom of translucent particles of a powder would decrease the albedo and strongly affect the other photometric properties.

##### 1. Effect of particle size

The rock selected in this experiment for detailed analysis is olivine basalt porphyry. This is a basic rock

and consists primarily of plagioclase feldspar and pyroxene. The material was pulverized in a tungsten carbide ball mill and separated into different size ranges by sieving, sedimentation and tube centrifuging. The size ranges used are: (1) less than  $1\mu$  (2)  $1-5\mu$  (3)  $5-10\mu$  (4)  $10-20\mu$  (5)  $20-37\mu$  (6)  $37-74\mu$  (7)  $74-149\mu$  (8)  $0.5-2\text{mm}$  (9) freshly broken surface. The various samples were separately poured on a glass plate and irradiated by 2 kev hydrogen ions for a dose of about  $90\text{ coul/cm}^2$ . The optical properties of each specimen were carefully measured using the photometer before and after the irradiation. Typical curves for  $1-5\mu$  and  $74-149\mu$  powders are shown in fig. 4 and fig. 5.

The manner in which particle size effects the various photometric characteristics of olivine basalt will now be discussed.

a. Albedo

Natural rock-forming minerals are not perfectly opaque; light penetrating into the interior of a grain is partly absorbed and partly re-emitted with reduced intensity. More light is absorbed by bigger particles due to the longer ray path, and a lower albedo results.

Before irradiation, the normal albedo  $B$  decreases monotonically with increasing size. After irradiation by H-ions, all materials having particle size below about  $150\mu$  are reduced in albedo, while for samples with particles greater than about  $0.5\text{m.m.}$  irradiation slightly increases

from  $1-5\mu$  to  $20-37\mu$  the albedo decreases, but for larger particle sizes the albedo increases with size. These results are shown in fig. 6.

b. Polarization

The positive polarization is higher for larger particles. The negative polarization for size greater than  $20\mu$  also increases with size, but for particles less than  $20\mu$ , it decreases with size (see fig. 7 and fig. 8), however, for particles less than  $1\mu$  the polarization increases again.

The increase of positive polarization with size can be understood as follows. As the particle size increases, more of the refracted light is absorbed. The light which is directly reflected from the surface is positively polarized, but the light which is refracted and scattered from the interior of translucent substances is negatively polarized; thus as the opacity of a substance is increased the net positive polarization is increased.

The cause of negative polarization at small phase angles is not understood. It is probably a result of multiple scattering (Öhman)<sup>(10)</sup> and interior refraction (Lyot)<sup>(8)</sup>. For irradiated surfaces, the negative polarization at small phase angles also become more pronounced. This behavior may be due to the etch pits produced by sputtering and to multiple reflection at edges of these etch pits.

The phase angles of maximum and minimum polarization are shifted toward larger angles for larger particles, and the angle of inversion decreases with size for less than  $20\mu$ . For particles bigger than  $20\mu$  the minimum and inversion angles seem to have no dependence on size, whereas the maximum angles are greater or equal to  $130^{\circ}$ , which is the maximum phase angle at which the photometer can reliably measure. H-ion bombardment changes the value of most optical parameters, but the relation between polarization and size remains similar.

c. Intensity

Following Orlova, <sup>(1)</sup> it is convenient to classify the reflection laws of various types of surfaces as follows: (1) diffusing surfaces, which approximately satisfy Lambert's Law, appearing equally bright in all directions; (2) specularly-reflecting ones, with maximum intensity in the direction opposite the incident ray; (3) completely rough ones with the maximum of reflection in the direction of the incident ray. It should be clear that the classifications of surface properties used here are not sharply-defined and that a continuous gradation exists between each category. The manner in which surfaces scatter light have been discussed in detail by B. Hapke and H. Van Horn; <sup>(2)</sup> it is governed by albedo, macroscopic and microscopic structure of the surface.



Of the surfaces investigated here, the three smaller ranges of sizes are conspicuously of type 3. Surfaces with particle size of 10-20 $\mu$  to 74-149 $\mu$  are of the second type; and freshly broken surfaces belong to the first type. H-ion irradiation has a strong tendency to sharpen the backscatter peaks of rough surfaces.

#### d. Color

Before irradiation the color is determined by the absorption properties of the rock, but after irradiation the dark coating controls the color. The dark coating evidently absorbs more blue light than red light. The positive polarization, which is related to albedo, is higher for blue than for red.

The color of the bombarded materials has a regular dependence on size (see fig. 9). The ratio of  $B_R/B_G$  decreases with size while  $B_B/B_G$  increases with size. If the intensity at ( $i = 58^\circ$ ,  $\epsilon = 60^\circ$ ,  $\phi = 2^\circ$ ) is set equal to unity, it is found that the relative intensity at ( $i = -30^\circ$ ,  $\epsilon = 60^\circ$ ,  $\phi = 90^\circ$ ) is generally proportional to wavelength (i.e., the sharpness of the backscatter peak decreases as  $\lambda$  increases); polarization at  $\phi = 90^\circ$  was found to vary inversely with wavelength.

#### 2. Effect of surface compaction

Surfaces of different compaction for less than 1 $\mu$ , 1-5 $\mu$  and 5-10 $\mu$  olivine basalt porphyry powders were prepared by pressing, pouring and sieving. The results, which

are given in fig. 10 - fig. 12, show that increasing the compaction increases both albedo and polarization for  $1-10\mu$ .

The absorption which accompanies every reflection is the reason why the albedo of the surface decreases with increasing porosity, for a typical ray of light must undergo more reflections in order to escape from a complex macro-structure. Reducing the compaction of the surface also allows more vertical surfaces to take part in the reflection process; hence, the positive polarization is reduced. The pressed surfaces behave like diffusing surfaces and give a Lambert-type Law. The surface of a poured powder is rough enough to produce a backscatter-type of curve. The sifted surface can be considered as a mixed specimen with two maxima: one in the direction of the incident ray and one opposite the incident ray. This sifted surface is sufficiently rough to have backscatter, but the loose packing permits refracted light to have more chance to go out in the specular direction.

For particles with size less than  $1\mu$  the surface-adhesive forces completely dominate the packing properties of the grains. These intergrain forces strongly agglomerate the grains and cause them to form clumps of low density. Thus the optical properties of these sized particles are controlled by the clumps rather than by individual grains.

### 3. Type of radiation

Effects of three types of radiation,  $\gamma$ -ray, 2 keV H ions and 2 keV He ions, were investigated in this experiment. Irradiation of all sizes of olivine porphyry by  $\gamma$ -rays for a dose of  $10^6$  roentgens produced no measurable change in their photometric properties. The irradiation by H ions and He ions drastically affects the optical properties of rock powders, as described above. The effects of He ions are similar to those of H ions except more produced. The variation of a few optical parameters with different type of irradiation are listed in Table 1.

Optical parameter Type of radiation	Albedo (%)	Pmin. (%)	Pmax. (%)	Scattering Law
unirradiated	$42.8 \pm 1.7$	$1.0 \pm 0.1$	$1.2 \pm 0.1$	wide backscatter
$\gamma$ -ray $10^6$ reogten	$41.8 \pm 1.7$	$1.0 \pm 0.1$	$1.0 \pm 0.1$	wide backscatter
H-ion 90 coul/cm <sup>2</sup>	$10.3 \pm 0.4$	$1.5 \pm 0.2$	$2.7 \pm 0.2$	sharp backscatter
He-ion 90 coul/cm <sup>2</sup>	$3.8 \pm 1.5$	$2.0 \pm 0.2$	$3.4 \pm 0.2$	sharp backscatter

Table 1. Effects of  $\gamma$ -ray, H-ion and He-ion on the optical properties of olivine basalt porphyry of size 1-5 $\mu$ .

#### 4. Dose of hydrogen ion irradiation

Increasing the dose of radiation to 1-5 $\mu$  olivine basalt porphyry by 2 kev H-ions shows that the photometric characteristics change monotonically with dose in the manner previously noted. For greater dose, the normal albedo decreases and approaches a saturation value around 5% (see fig. 13). An enhancement of negative and positive polarization, and a sharpening of backscatter also results from prolonged irradiation. The ratio  $B_B/B_G$  decreases and  $B_R/B_G$  increases with the increasing dose; this is shown in fig. 14. Every parameter seems to have been saturated by 300 coul/cm<sup>2</sup> except possibly the positive and negative polarization peaks. (fig. 15)

#### 5. Composition

In order to determine the effect of varying the chemical composition of the samples, different types of igneous rock powders with a particle size less than 10 $\mu$ , were investigated. The rocks were obtained from Ward's Natural Science Establishment, Rochester, N. Y. The rocks used were nepheline syenite, rhyolite, olivine basalt porphyry and dunite. The photometric characteristics of the rock powders studied in this experiment are shown in figures 18-23.

Generally speaking, in large pieces acidic rocks are lighter in color than basic rocks; but this is not true for materials in which the particle size is less than 10 $\mu$ . For

instance, powdered nepheline synte, which is an acidic rock, has an albedo of 41%, while powdered dunite, a basic rock, has a higher albedo of 53%. However, a regular relation exists between the composition of irradiated rock powders and their photometric properties. No matter how high the albedo of the unirradiated surface, basic powders have lower albedo after irradiation than acidic rock powders. The basic rocks are richer in ferromagnesium minerals and poorer in silica. Positive and negative polarization also vary with composition.

Tektites<sup>(12)</sup> and volcanic<sup>(13)</sup> ash have been suggested as possible materials on the lunar surface; hence samples of these substances have also been studied. There are no special difference between the photometric properties of tektite powders and pulverized volcanic ash and those of other igneous powders. The surfaces of these powders after irradiation are shown in fig. 16-17.

## V. APPLICATIONS TO THE MOON

This experiment differs in one important respect from conditions on the lunar surface in that the laboratory specimens were bombarded from the vertical, whereas the flux of solar wind particles impinging on the lunar soil is probably isotropic. This lack of isotropic bombardment causes the laboratory sample to be somewhat brighter when viewed and illuminated from large angles to the surface normal than when viewed and illuminated from the vertical. It also causes the polarization versus phase angle curves to be slightly different for  $\epsilon = 0^\circ$  than for  $\epsilon = 60^\circ$ . However, the isotropy of the lunar radiation conditions should remove these disparities; and during subsequent experiments in which the specimens were tilted back and forth during irradiation the photometric properties were indeed observed to become nearly independent of direction. (14)

The parameters investigated in this experiment are important to an interpretation of the optical properties of the lunar surface. Natural rocks are filled with imperfections and impurities which dominate their optical properties and hence these properties are not grossly different from one igneous rock to another. The quantitative differences in optical properties for various types of rocks should not significantly affect the conclusions of this paper which are based on olivine basalt powders.

Only irradiated materials with particle sizes less than about  $10\mu$  are capable of having several optical properties similar to those of the moon. On the lunar surface such fine powder would probably result from micrometeorites repeatedly impacting the surface of the moon.

Comparing the backscatter peak for powders of different compaction, the moon appears to be covered with a generally rough and moderately compacted surface similar to that which can be prepared by pouring a fine powder in the laboratory. The 'fairly castle' structure proposed by B. Hapke,<sup>(2)</sup> which is produced by sifting, has too much forward scatter for irradiated rock powders; it also seems rather artificial and might be hard to build by natural causes.

The solar wind-irradiation of the lunar surface appears to be capable of accounting for the low albedo and high polarization of the moon. The dose of H-ion irradiation necessary to provide lunar-like photometric properties is about  $100 \text{ coul/cm}^2$ , which is probably equivalent to around  $2 \times 10^5$  years on the moon. The question arises, why the moon with such a long life time (about  $4.5 \times 10^9$  years) has not had its photometric characteristic saturated under this continuous weathering process? This answer is probably that the lunar surface is continuously battered by micrometeorites; these impacts have the effect of stirring up and turning over the surface layer and continuously exposing fresh materials.

By suitable adjustment of the particle size and dose of irradiation many kinds of rock powders can probably be made to have optical properties similar to those of the moon. Thus this work supports the hypotheses that the difference in photometric properties between various lunar features, such as the darker mares and brighter highlands and craters, is due to variations in chemical composition or to different time of exposure to the solar-wind. The mare regions, characterized by low albedo, high polarization and narrow backscatter peak, may be covered by an absorbing, opaque layer of powders, having a constitution similar to that of basic rocks. Prolonging the time of irradiation also leads to the mare-type of photometric properties. On the other hand, one might think that the areas on the moon which are lighter and less intense in backscatter peak and polarization, consist of more acidic fine powders, or alternately have a shorter time of exposure to the solar radiations.



## VI. SUMMARY

The photometric and polarometric properties of rock powders are critically dependent on particle size and H-ion irradiation dose; surface compaction and chemical composition have less effect. With respect to the lunar surface, a moderately-compacted, powdered surface with a particle size distribution which peaks between 1 and 10 $\mu$  and irradiated by H-ions for a dose about 90 coul/cm<sup>2</sup>, possesses optical properties similar to those of the moon. Varying the chemical composition changes the optical curves slightly; however, it appears that by suitable minor adjustments of size distribution and dose, one can obtain the lunar-type curves from many different types of rock powders. It is not possible from these experiments to decide whether the different photometric characteristics of the mares, highlands and craters are primarily due to differences in chemical composition or to different times of exposure to the solar wind.

## REFERENCES

1. Wesselink, A. J., 1948, Bull. Astro. Insts. Neth., 10, 356.
2. Hapke, B., and H. Van Horn, 1963, 'Photometric Studies of Complex Surfaces, with Applications to the Moon', Jour. Geophys. Res., 68, pp. 4545-4570.
3. Hapke, B., 1964, The Lunar Surface Layer, J. Salisbury and P. Glaser, Ed., Academic Press, New York and London, p. 323.
4. Fesenkov, V. G., 1962, Physics and Astronomy of the Moon, Z Kopal, Ed., Academic Press, N. Y., p. 121.
5. Hapke, B., 1964, 'Effects of a Simulated Solar Wind on the Photometric Properties of Rocks and Powders', Center for Radiophysics and Space Research, Report No. 169, Cornell University, Ithaca, N. Y.
6. Wehner, G., C. Kenknight, and D. Rosenberg, 1963, 'Modification of the Lunar surface by the Solar Wind Bombardment', Planet. Space Science., 11, p. 1257-1261.
7. Neugebauer, M., and C. W. Snyder, 1962, 'The Mission of Mariner II, Preliminary Observations, the Solar Plasma Experiment', Science, 138, 1095-1096.

8. Lyot, B., 1964, 'Research on the Polarization of Light from Planets and from some Terrestrial Substances' Ann. Obs. Paris, 8, No.2, p. 127, English translation NASA TTF-187.
9. Handbook of Chemistry and Physics, 1959-1960, 41st Edition, pp. 2955.
10. Öhman, Y., 1950, 'A Tentative Explanation of the Polarization in Diffuse Reflection', Stock. Obs. Ann. Vol. 18, No. 8.
11. Orlova, N. S., 1962, Physics and Astronomy of the Moon, Z. Kopal, Ed., Academic Press, N. Y., p. 125.
12. O'Keefe, J., 1957, 'Lunar Rays', Astrophys. Jour., 126, p. 466.
13. Dollfus, A., 1962, Physics and Astronomy of the Moon, A. Kopal, Ed., Academic Press, N. Y., p. 125.
14. Hapke, B., 1965, Private Communication.

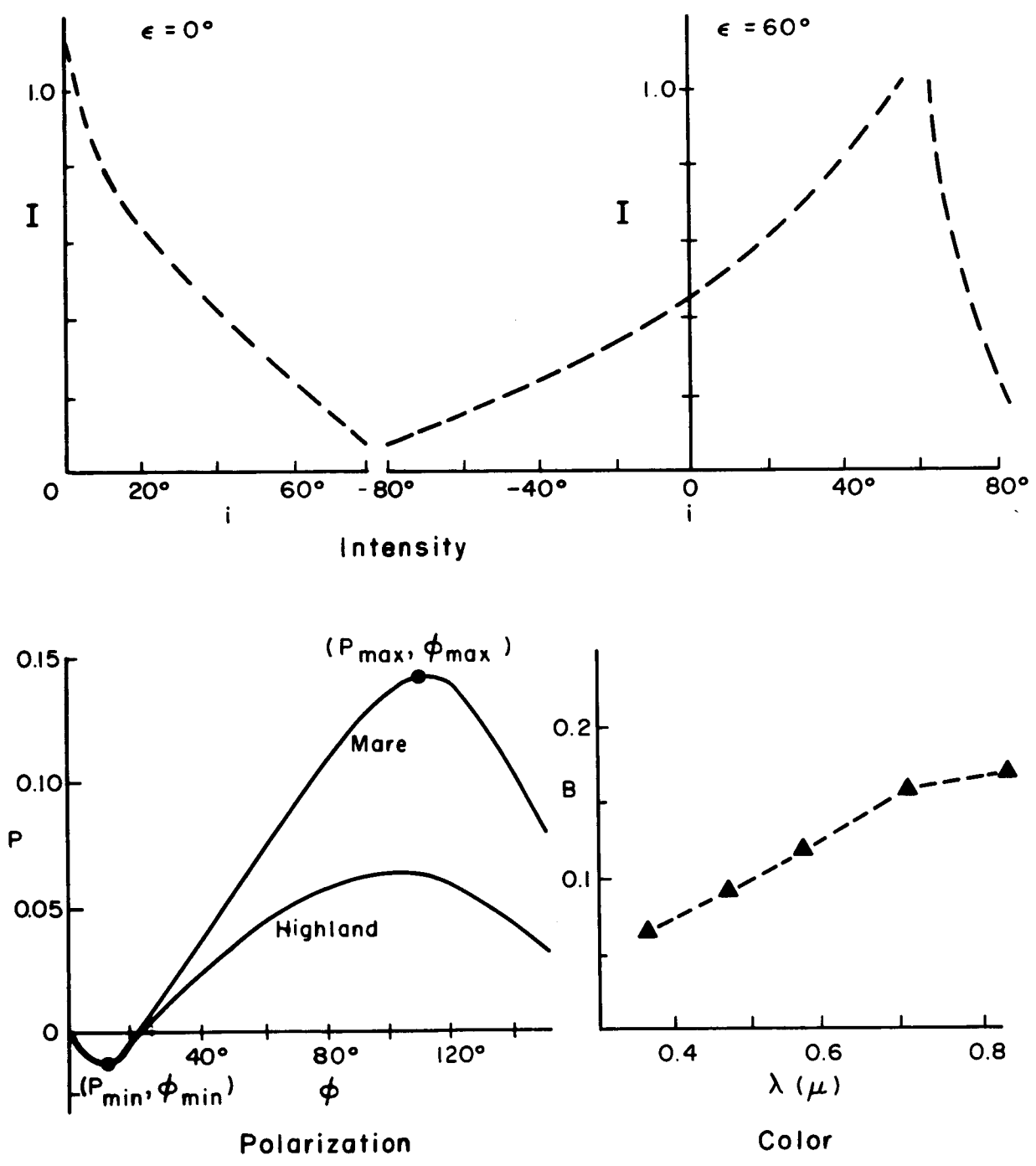


FIGURE 1. Typical curves of photometric characteristics of the lunar surface. The shapes of the polarization curves are nearly independent of angle of observation  $\epsilon$ .

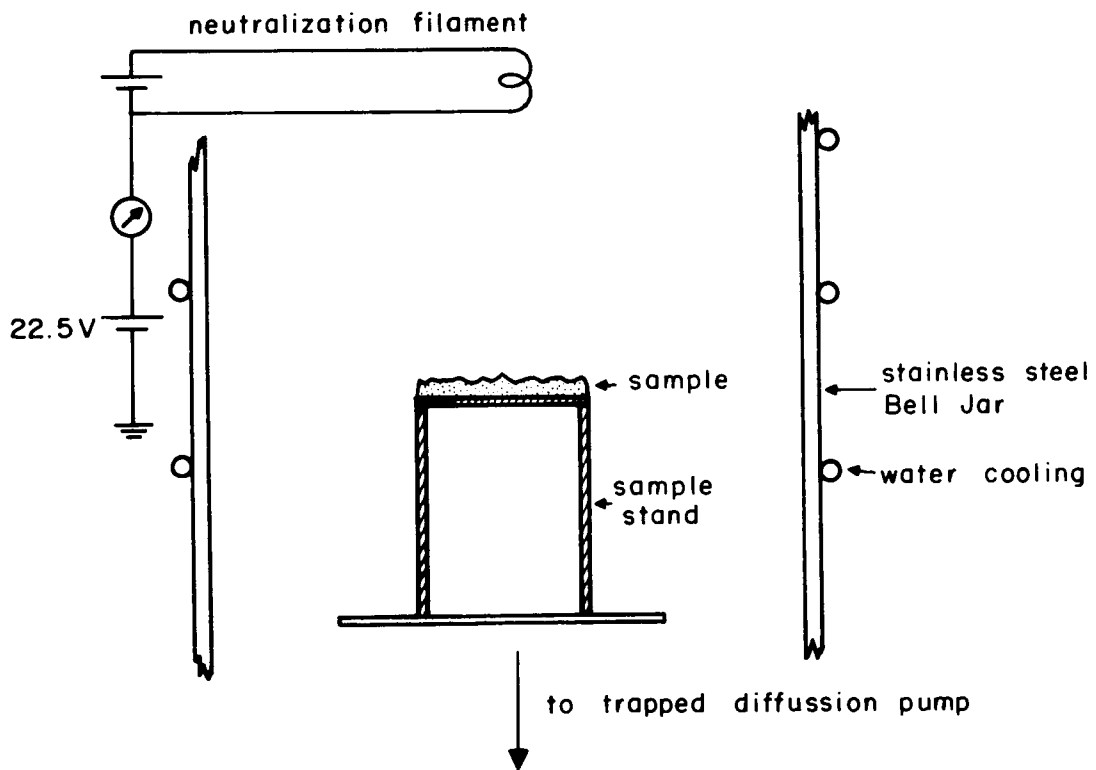
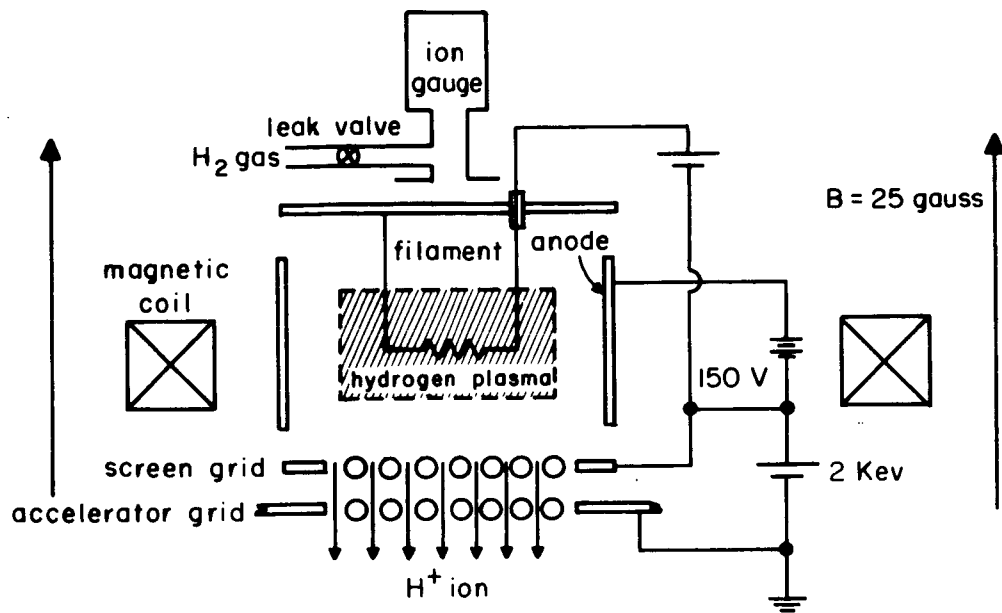


FIGURE 2. Ion gun schematic

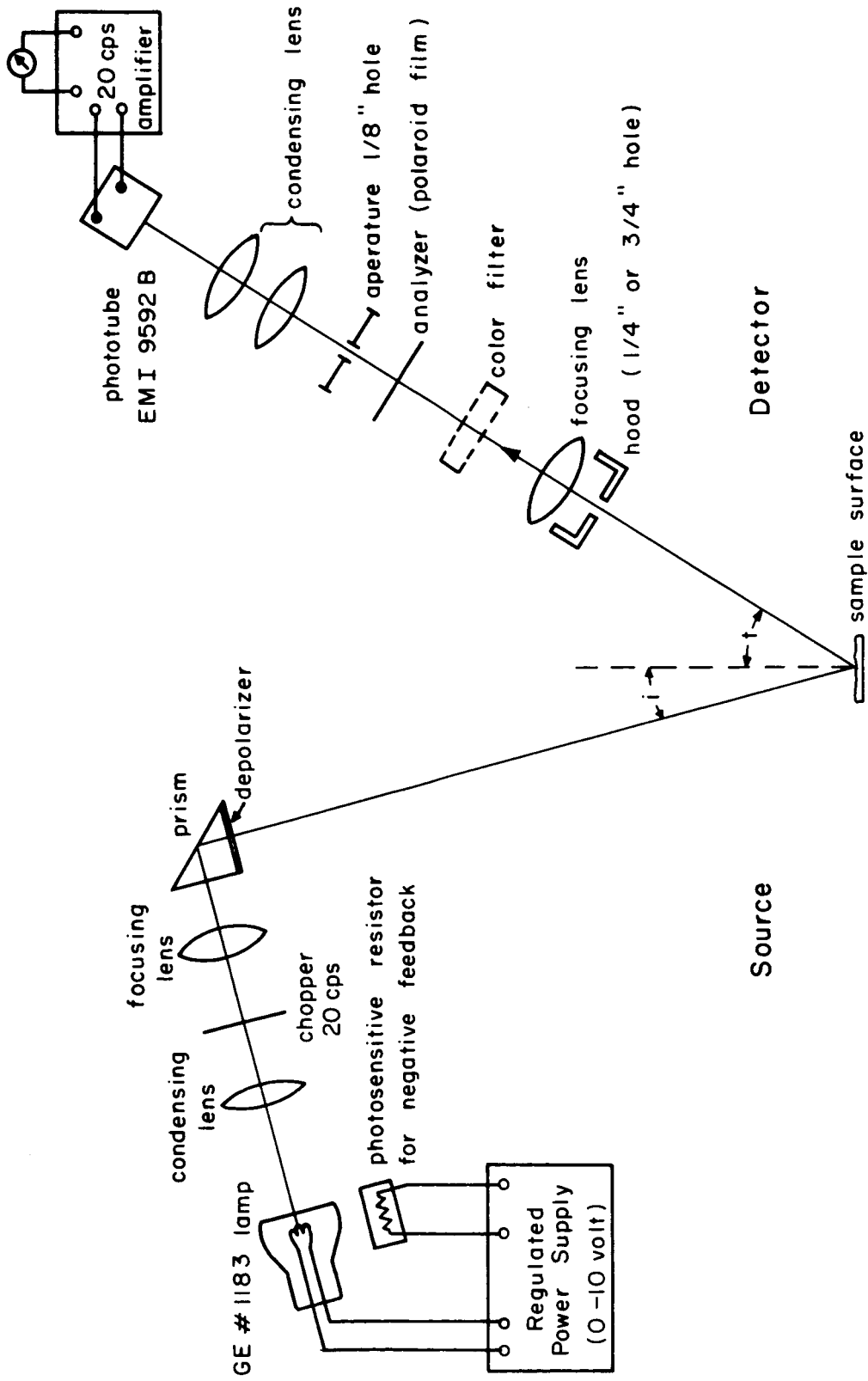


FIGURE 3. Photometer schematic

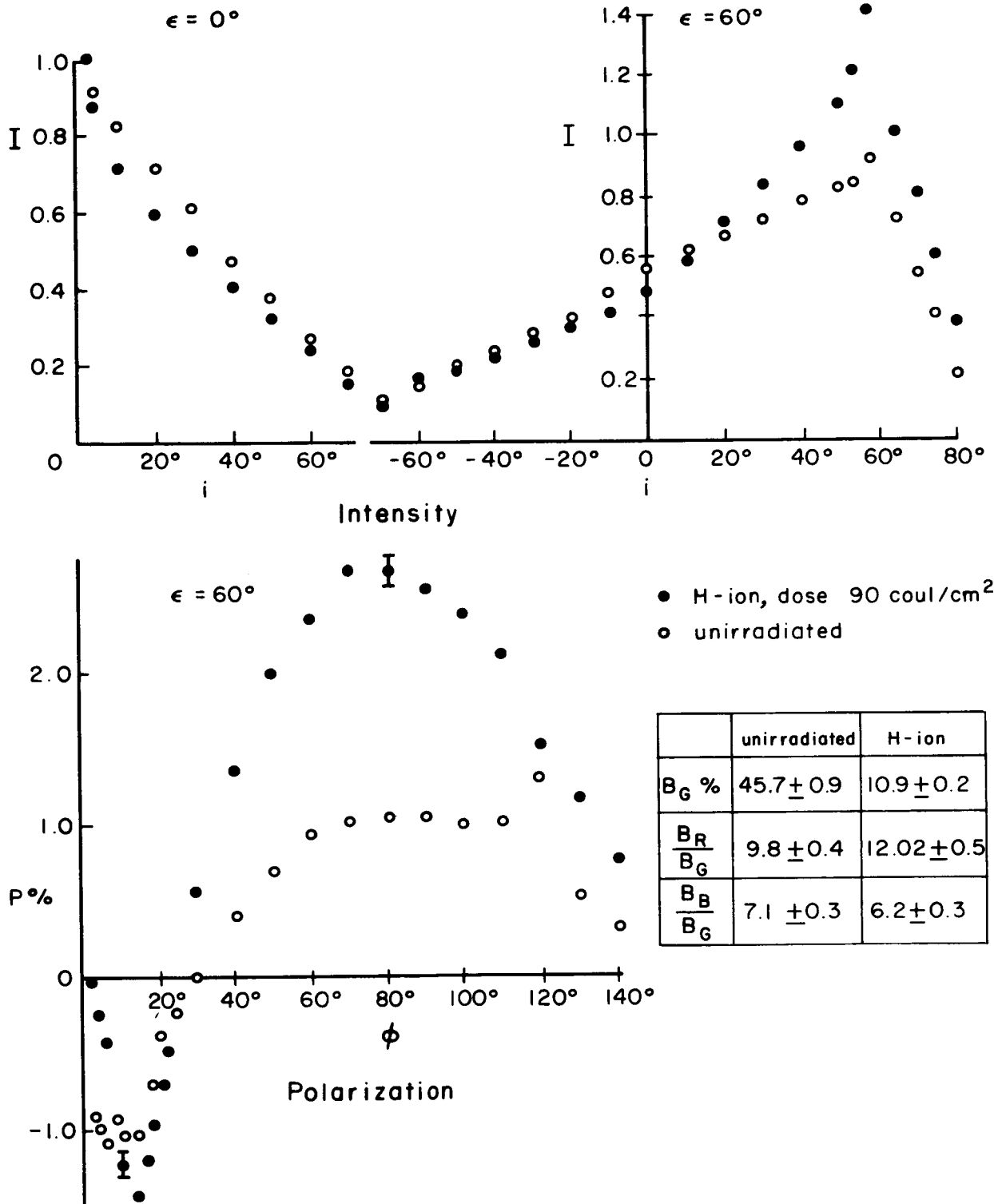


FIGURE 4. Photometric characteristics of olivine basalt powder of particle size 1-5 $\mu$ . Only polarization data for  $\epsilon = 60^\circ$  are shown; however, there is very little difference between the curves for  $\epsilon = 60^\circ$  and  $\epsilon = 0^\circ$ . (The anomalous polarization at  $\phi = 120^\circ$  is believed to be due to a small amount of specular reflection from the glass substrate holding the powder and is probably not significant.) The intensity curves have all been normalized to unity at ( $\epsilon = 0^\circ$ ,  $i = 2^\circ$ ).

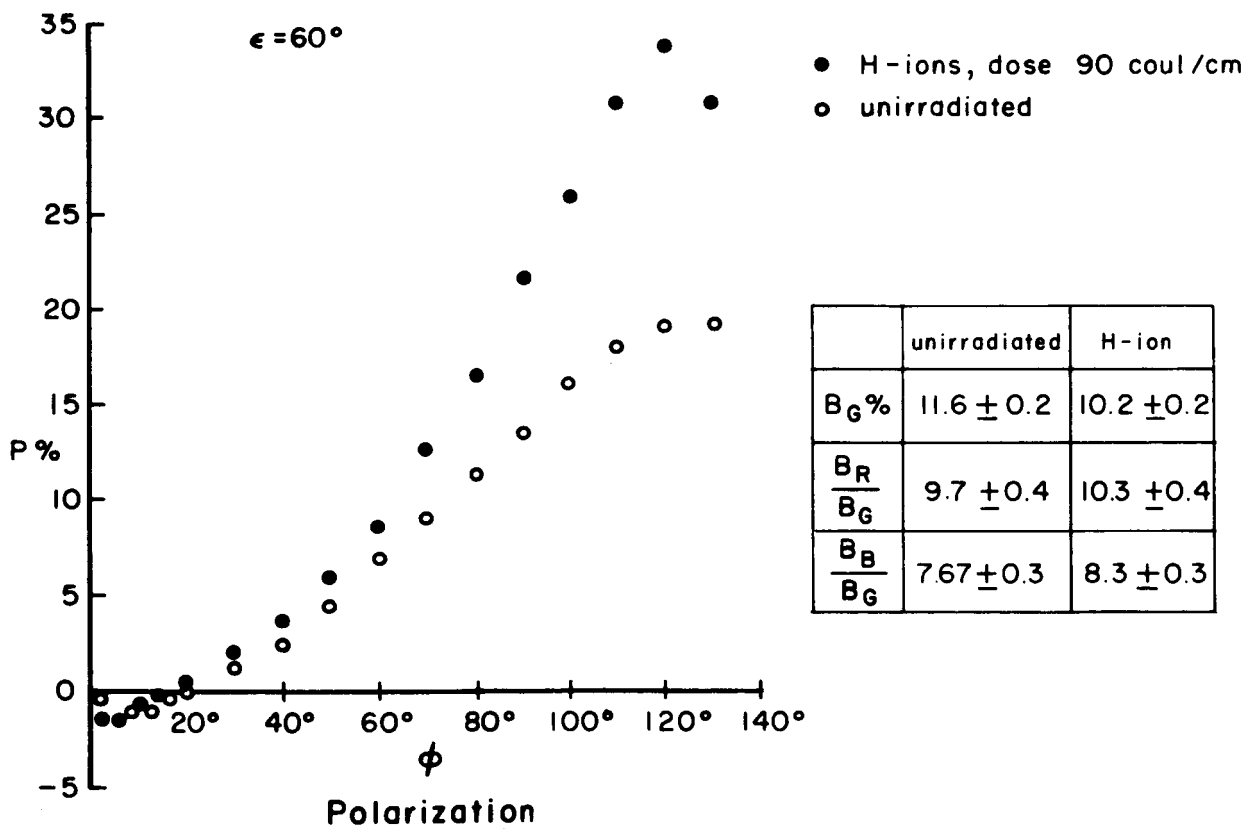
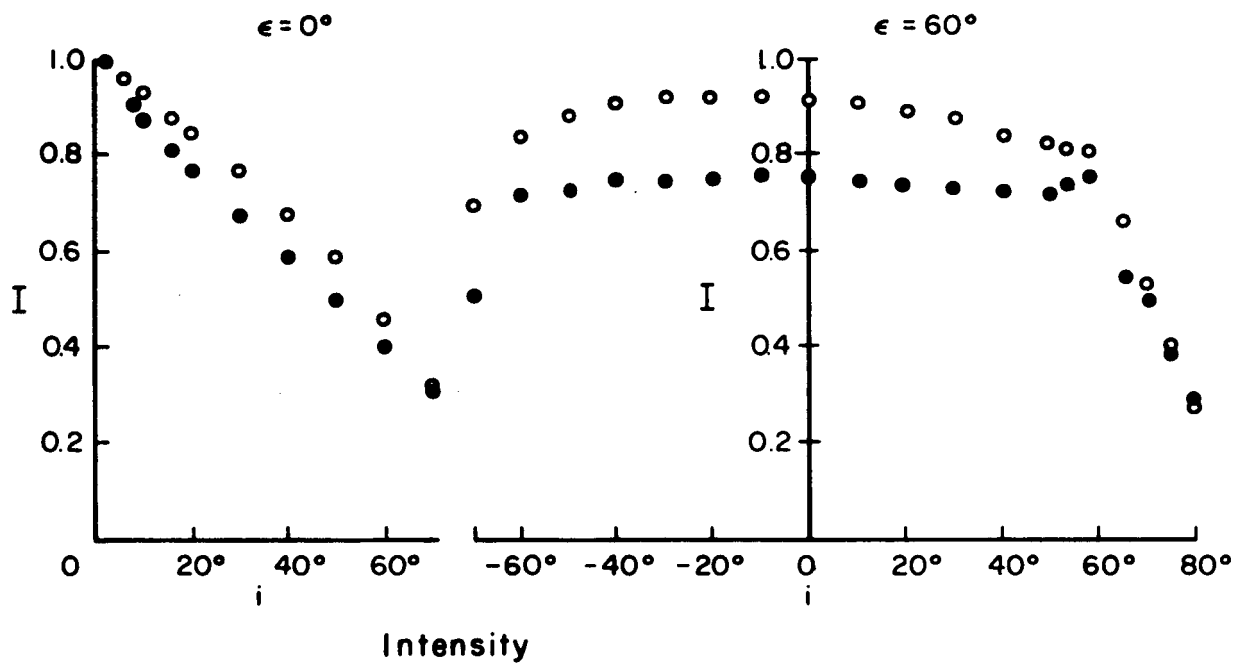


FIGURE 5. Olivine basalt porphyry (74 - 149 $\mu$ ).



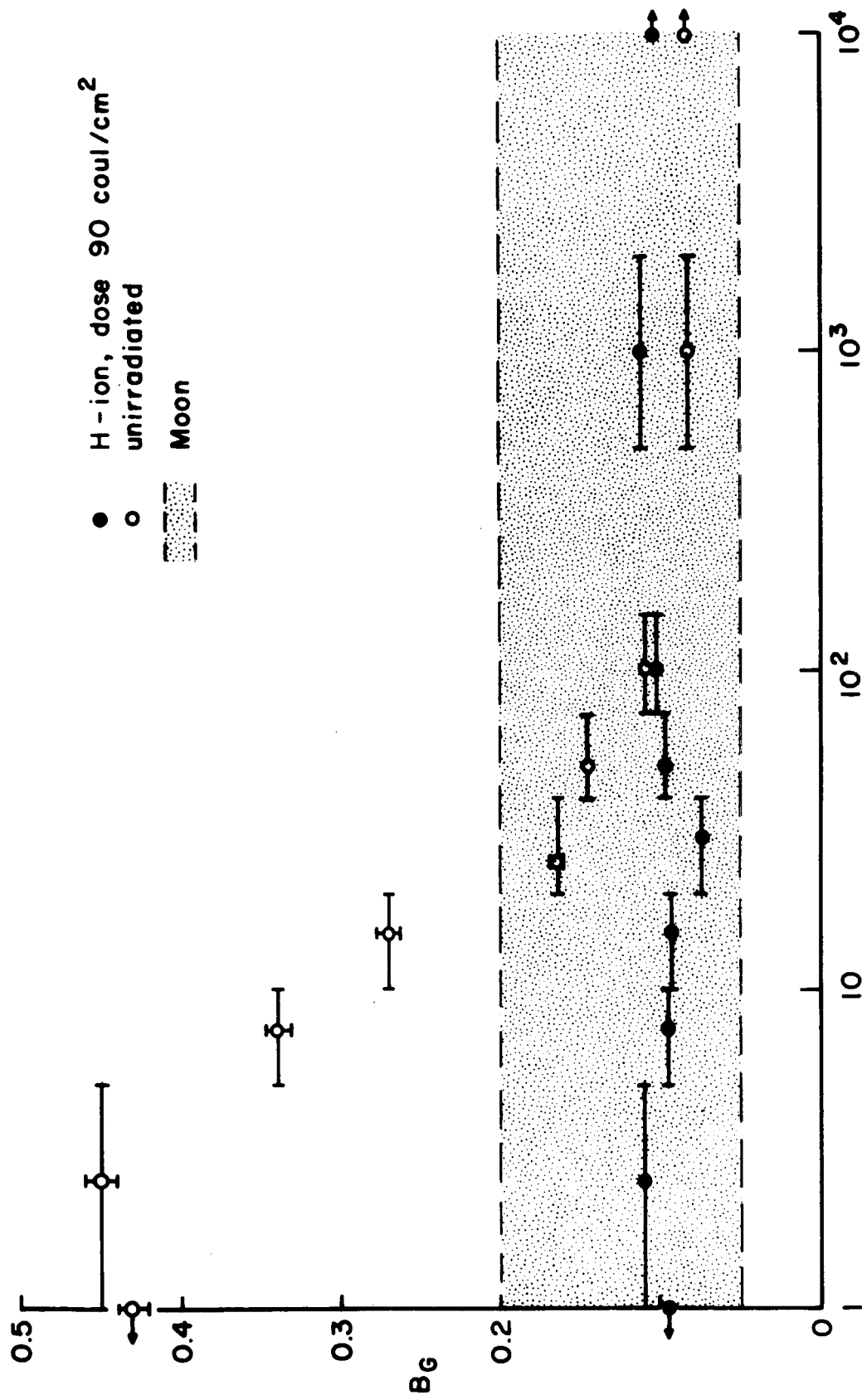


FIGURE 6. Normal albedo vs particle size. For convenience the freshly broken surface is shown as  $10^4 \mu$  in size.

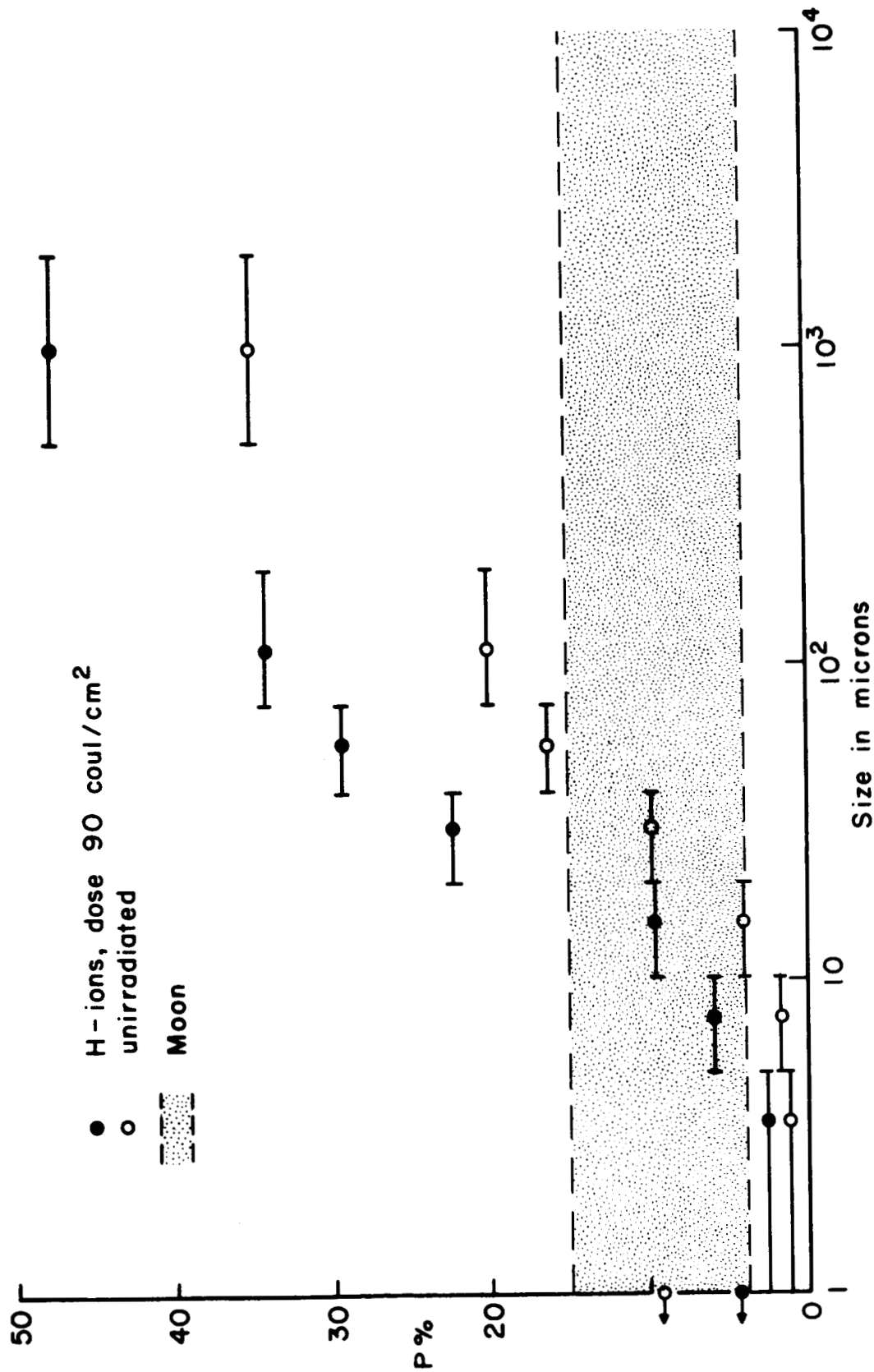


FIGURE 7. Maximum polarization vs particle size.

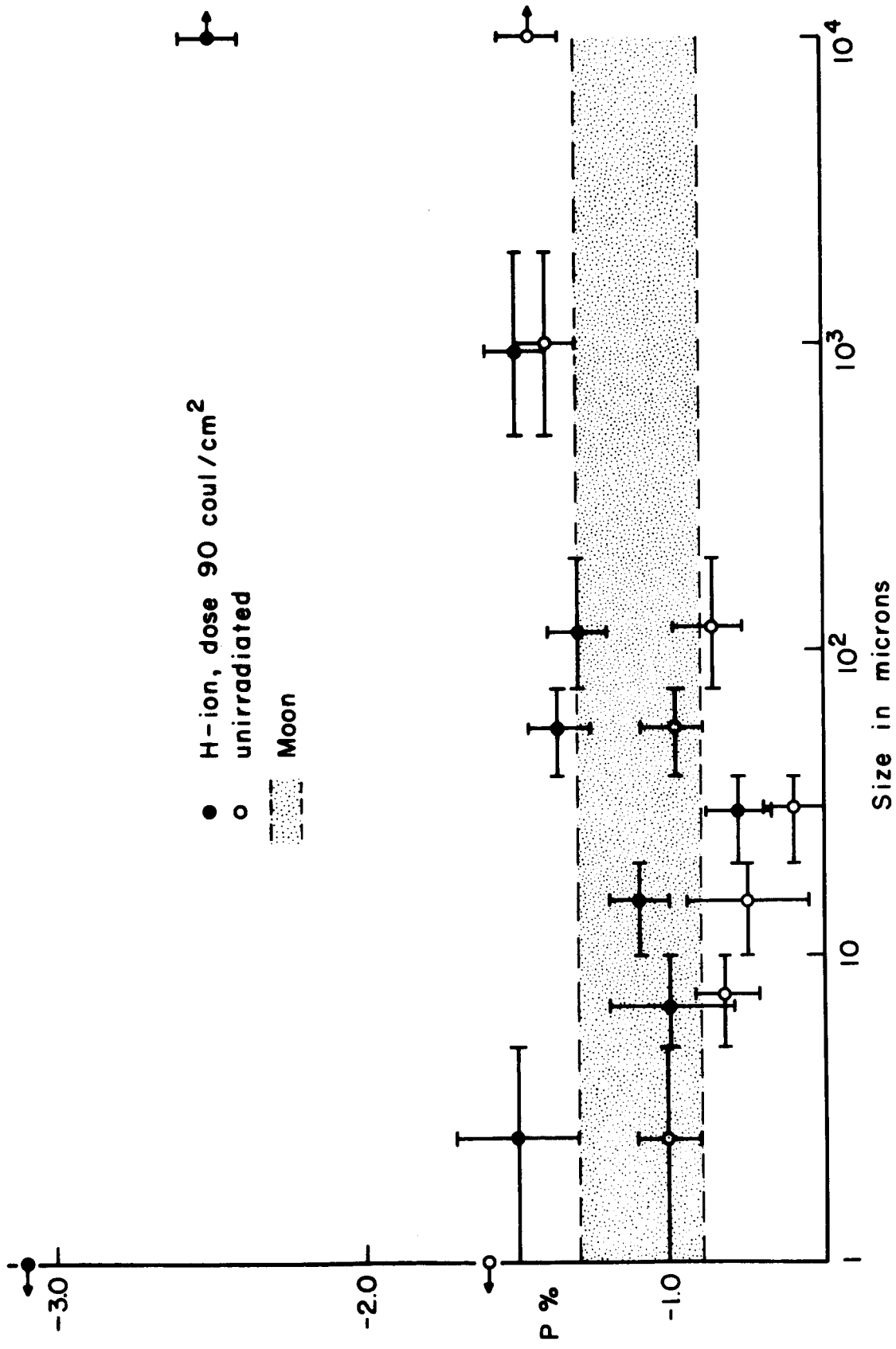


FIGURE 8. Minimum polarization vs particle size.

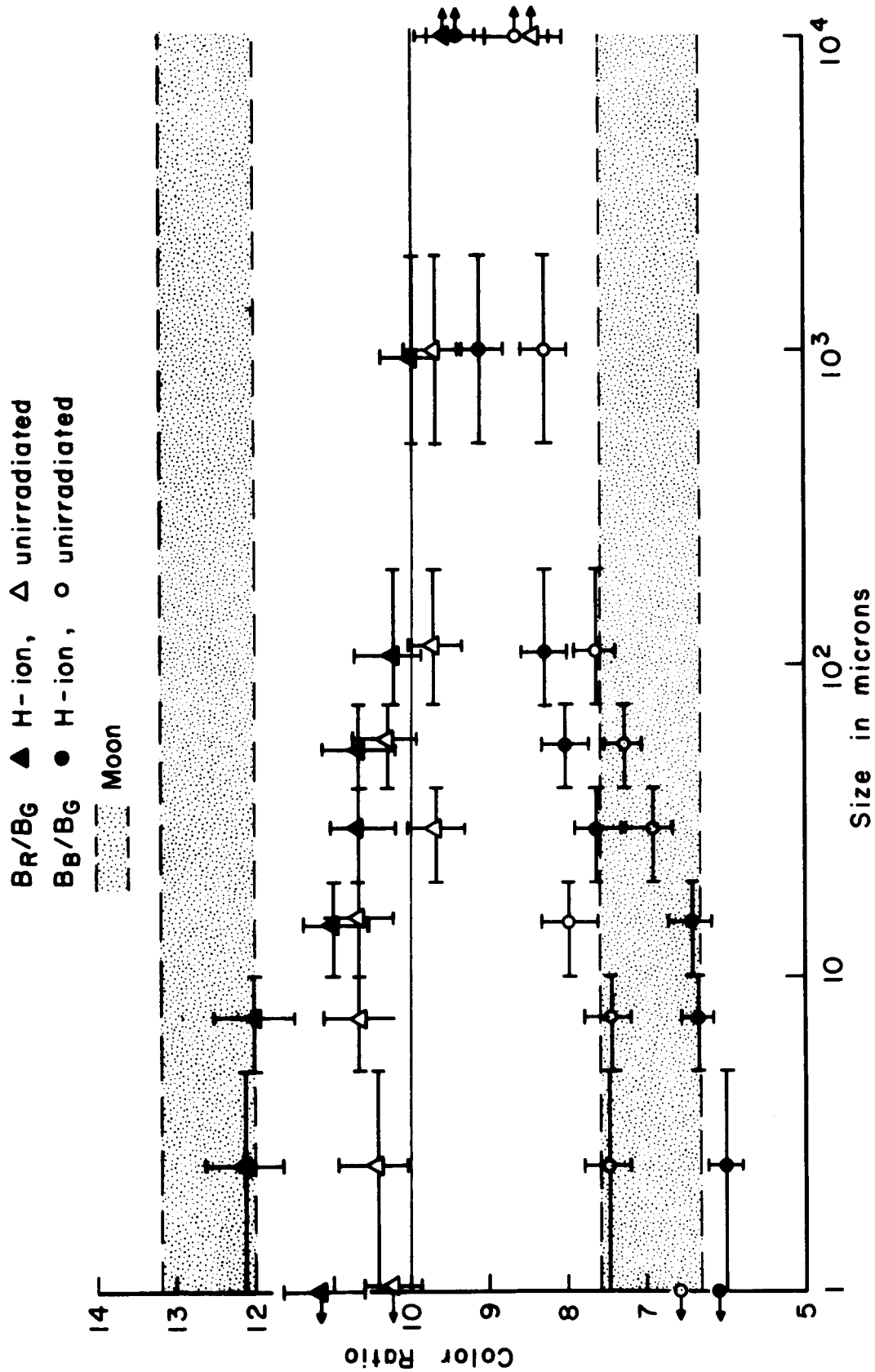


FIGURE 9. Color vs particle size.

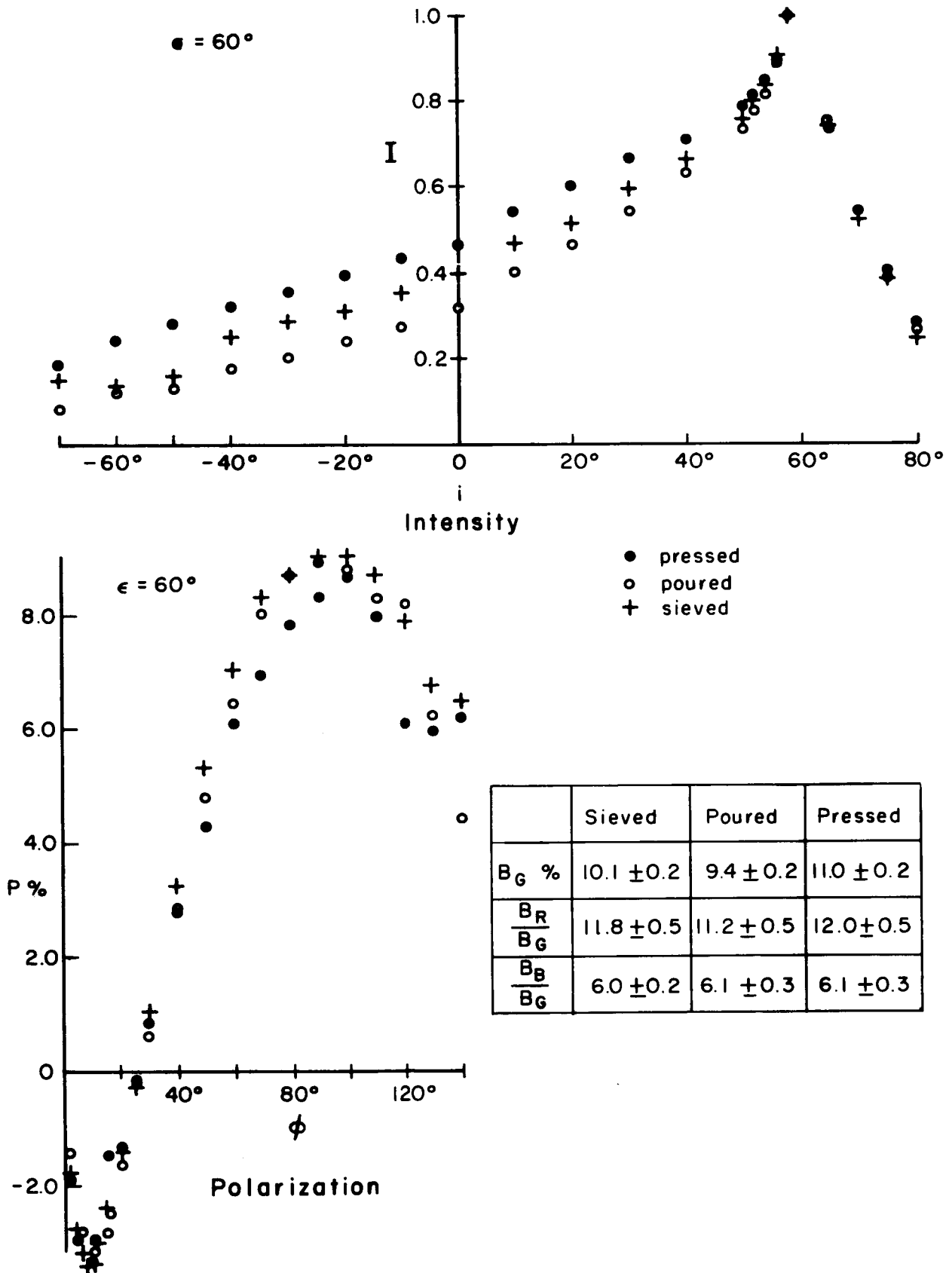
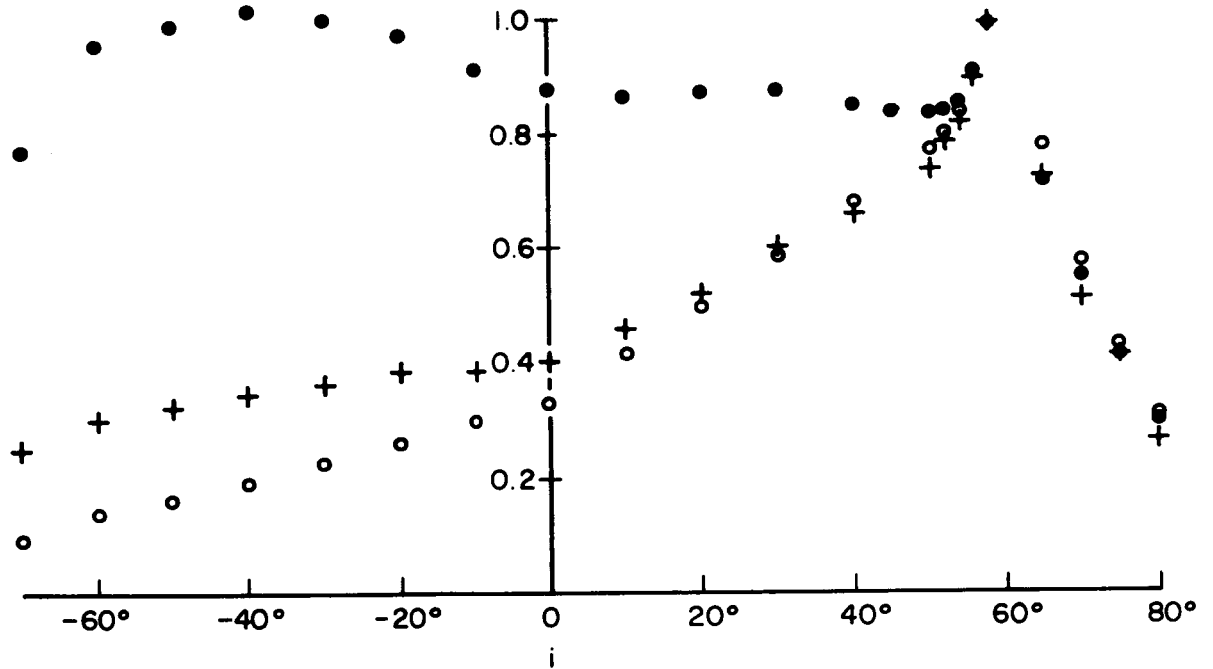
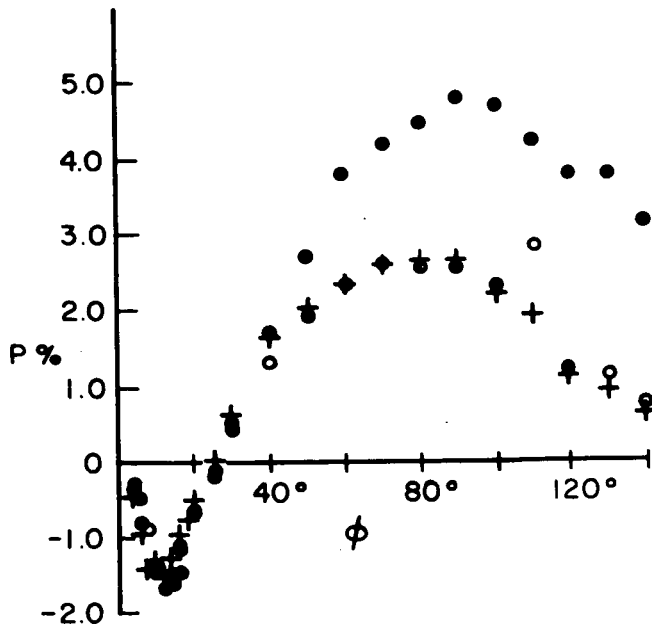


FIGURE 10. Effect of surface compaction on the optical properties of irradiated olivine basalt powder of size  $< 1\mu$ .



Intensity

- pressed
- poured
- + sieved



Polarization

	Sieved	Poured	Pressed
$B_G \%$	$9.3 \pm 0.2$	$10.9 \pm 0.2$	$15.2 \pm 0.3$
$\frac{B_R}{B_G}$	$12.2 \pm 0.5$	$12.2 \pm 0.5$	$12.1 \pm 0.5$
$\frac{B_B}{B_G}$	$7.5 \pm 0.3$	$6.0 \pm 0.2$	$5.9 \pm 0.2$

FIGURE 11. Effect of surface compaction on the optical properties of H-ion irradiated olivine basalt powder of size 1-5 $\mu$ .

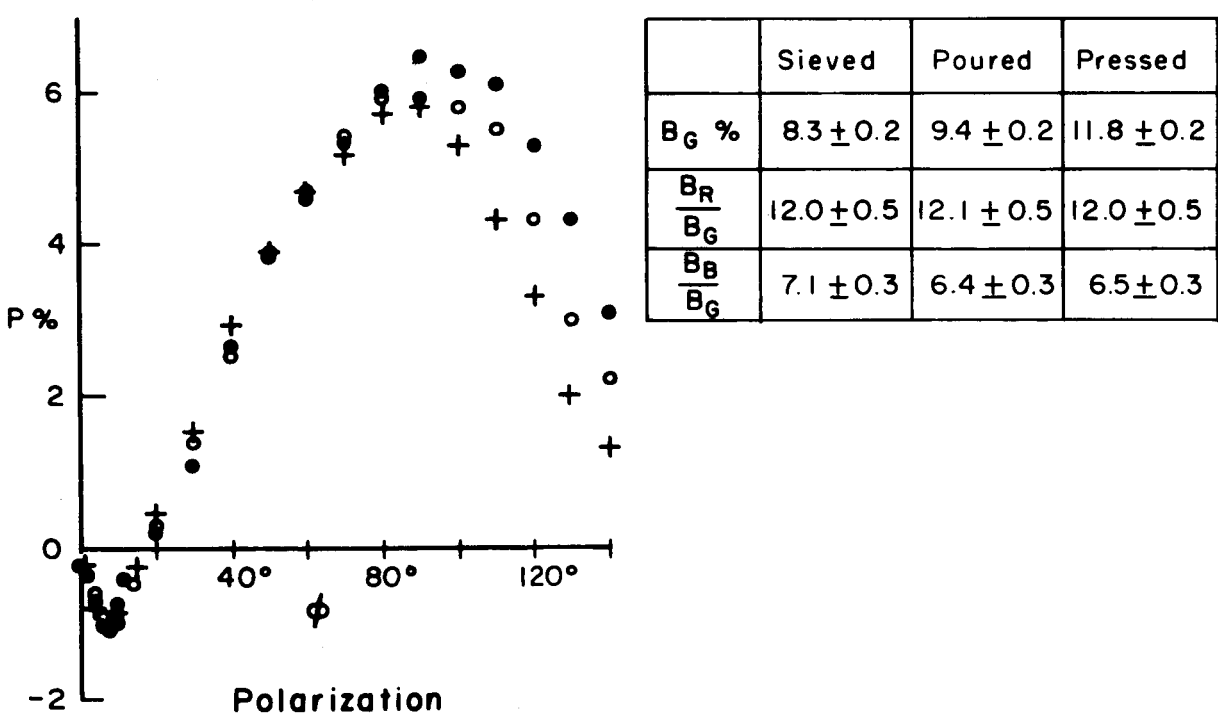
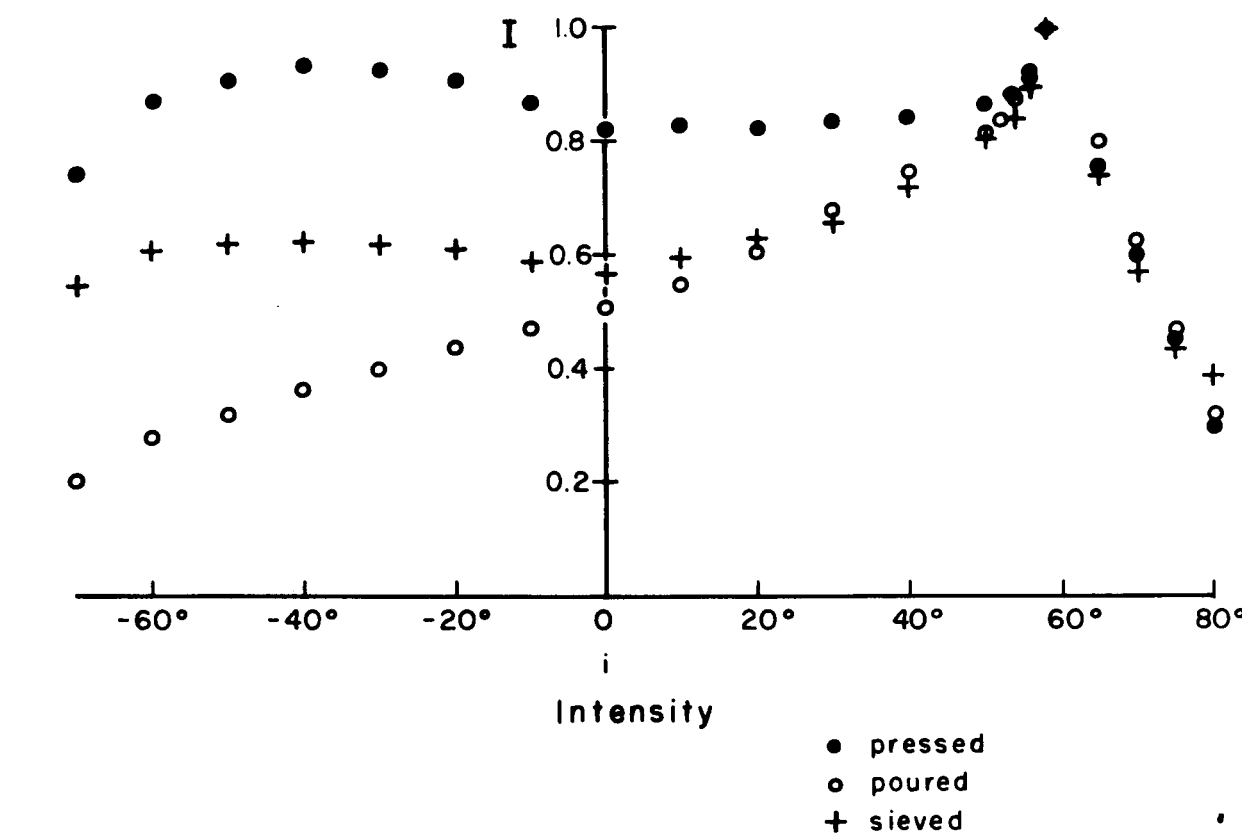


FIGURE 12. Effect of surface compaction on the optical properties of H-ion irradiated olivine basalt powder of size 5-10 $\mu$ .

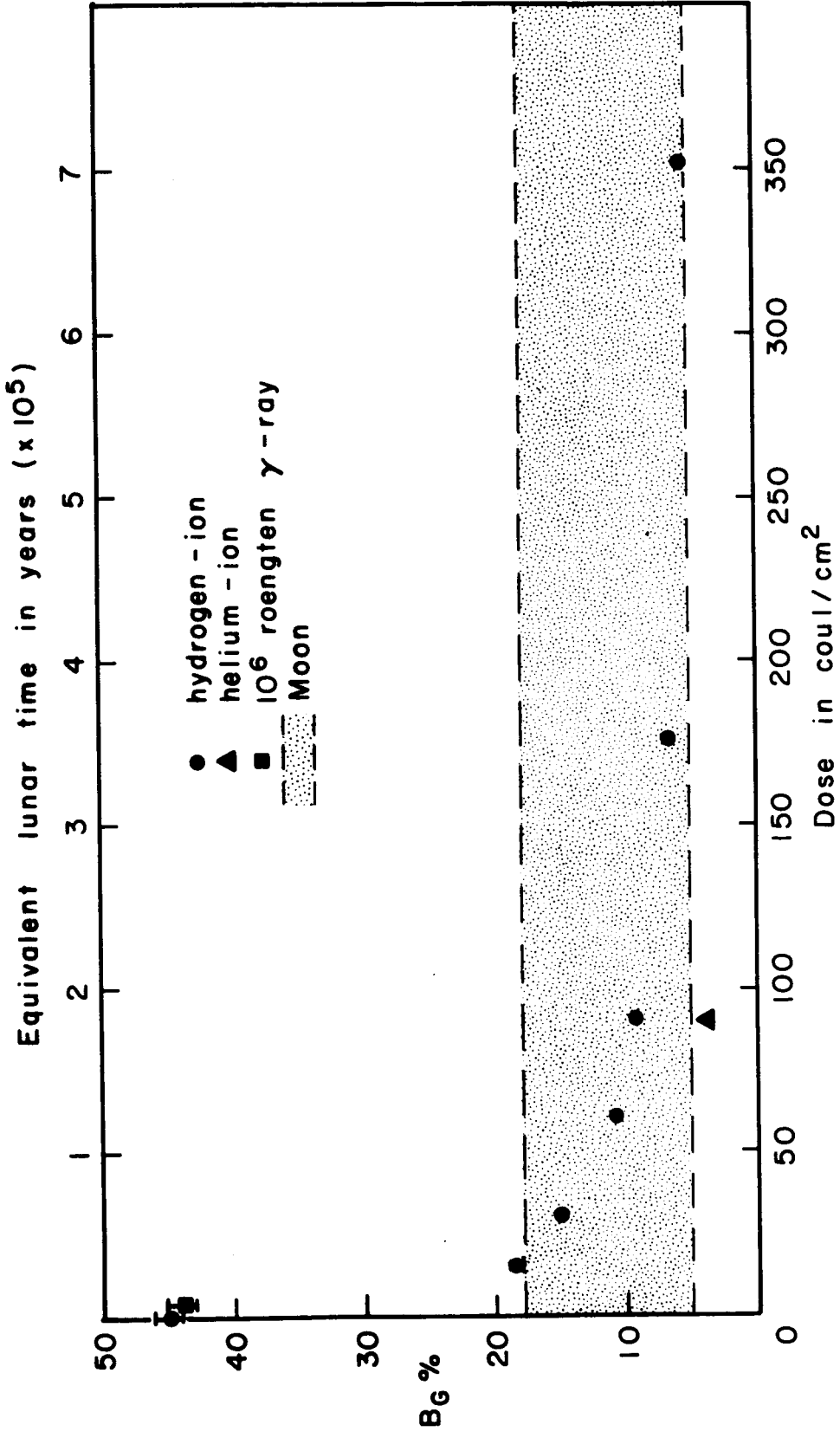


FIGURE 13. Normal albedo vs H-ion dose for olivine basalt powder of size 1-5 $\mu$ . The effects of  $\gamma$ -ray and He-ion irradiation are also shown.



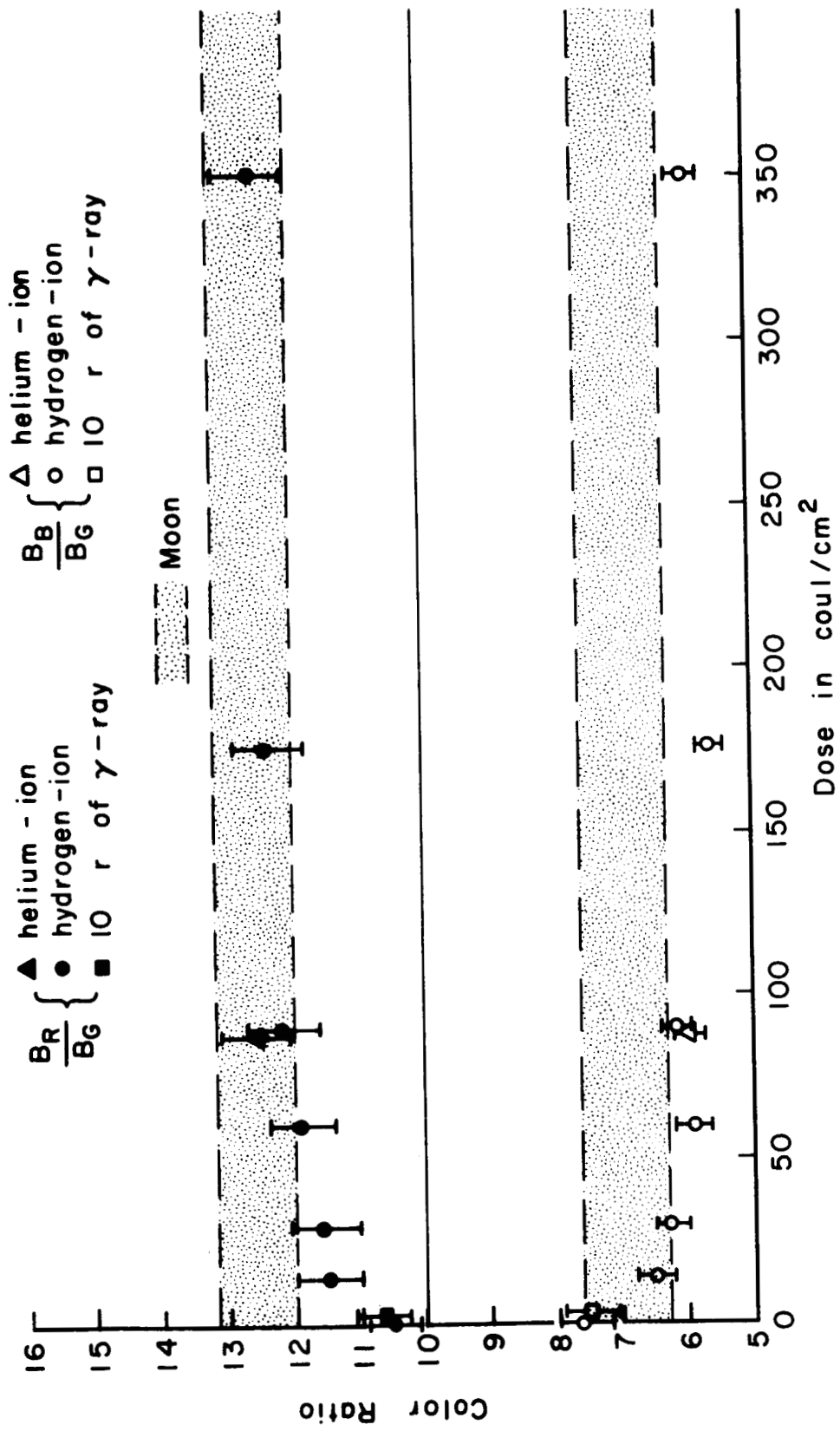


FIGURE 14. Color ratios vs H-ion dose for olivine basalt powder of size 1-5 $\mu$ .

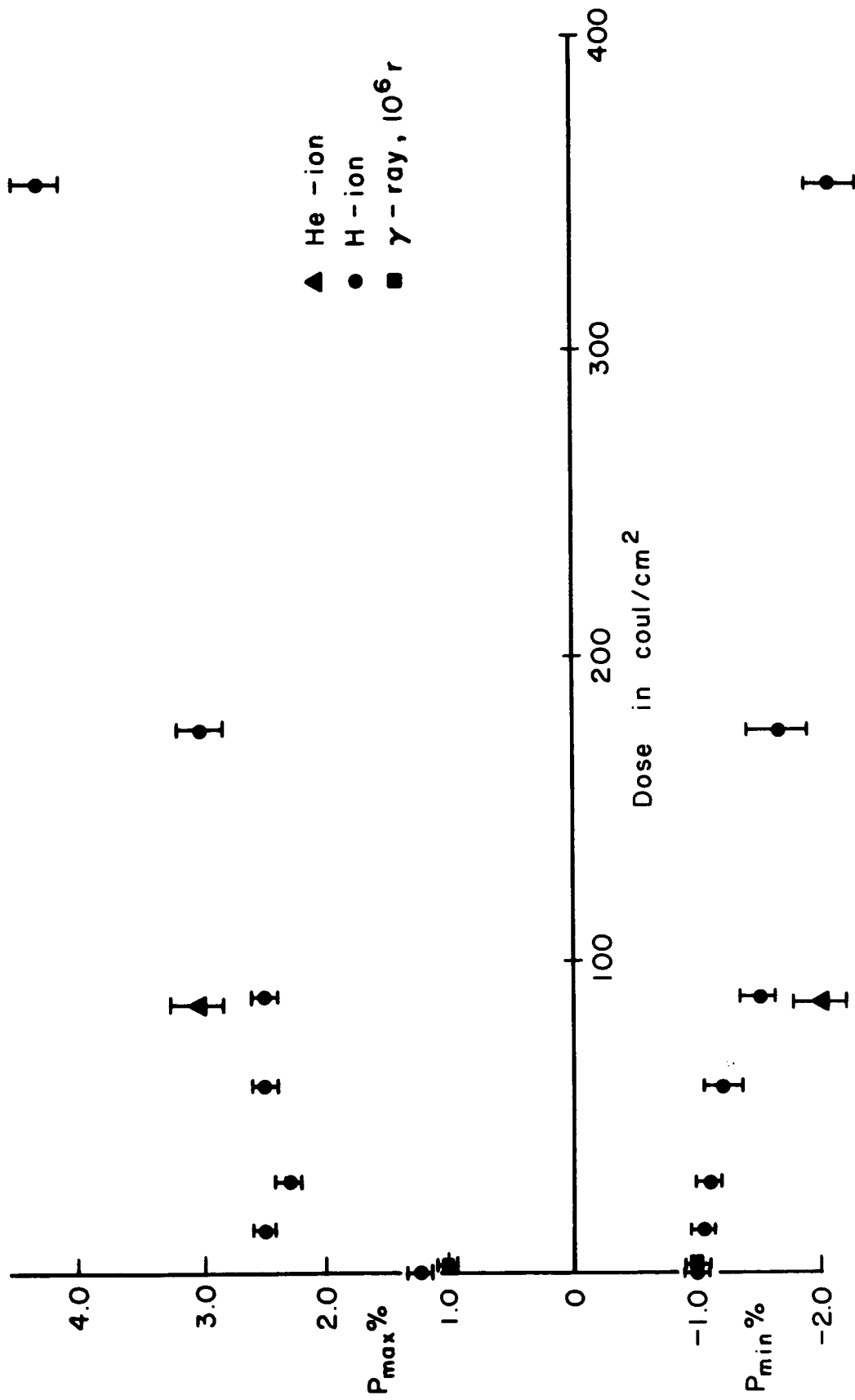


FIGURE 15. Maximum and minimum polarization vs H-ion dose for olivine basalt powder of size 1-5 $\mu$ .

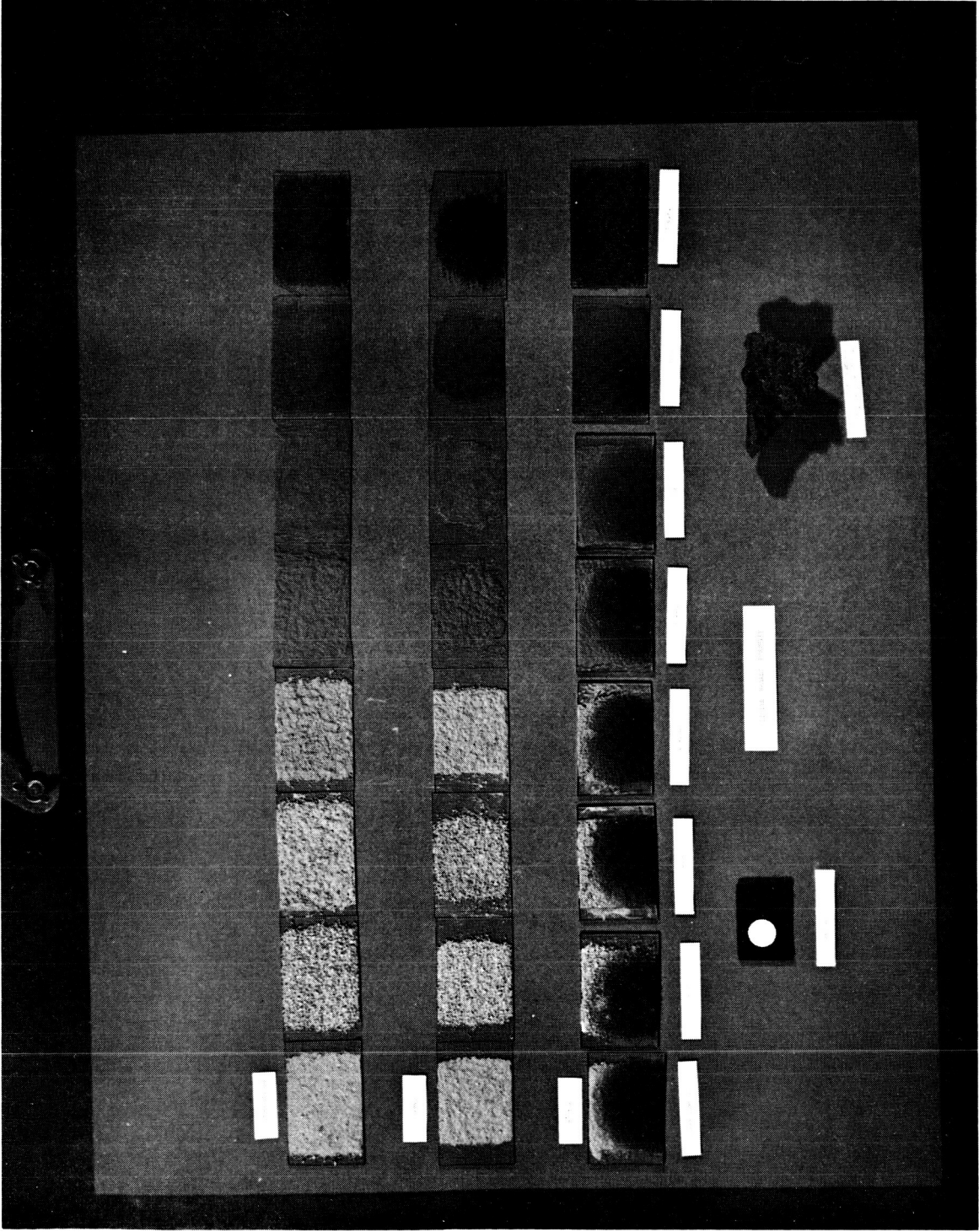


Figure 16. Photograph of olivine basalt powders.

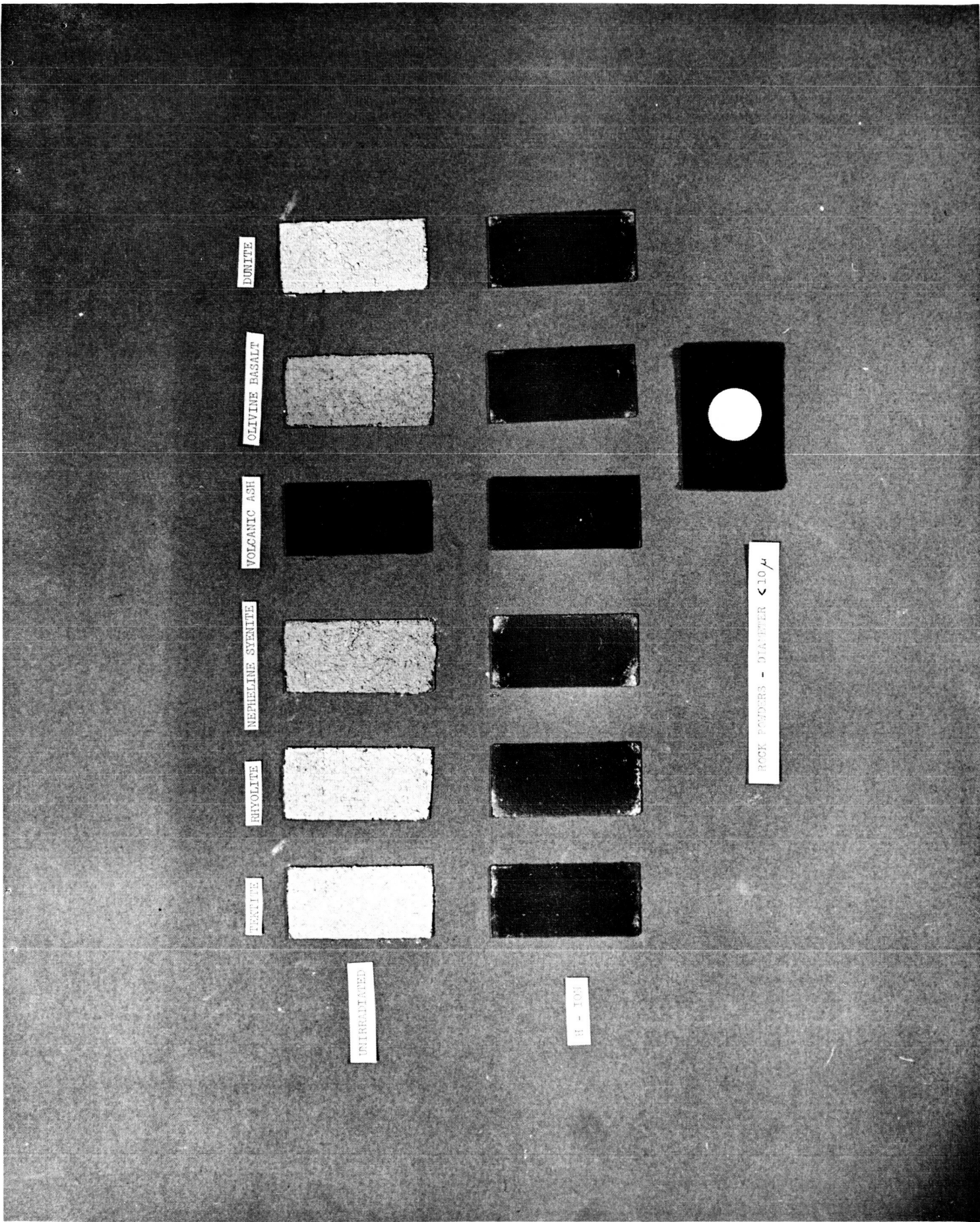


Figure 17. Photograph of igneous rock powders.

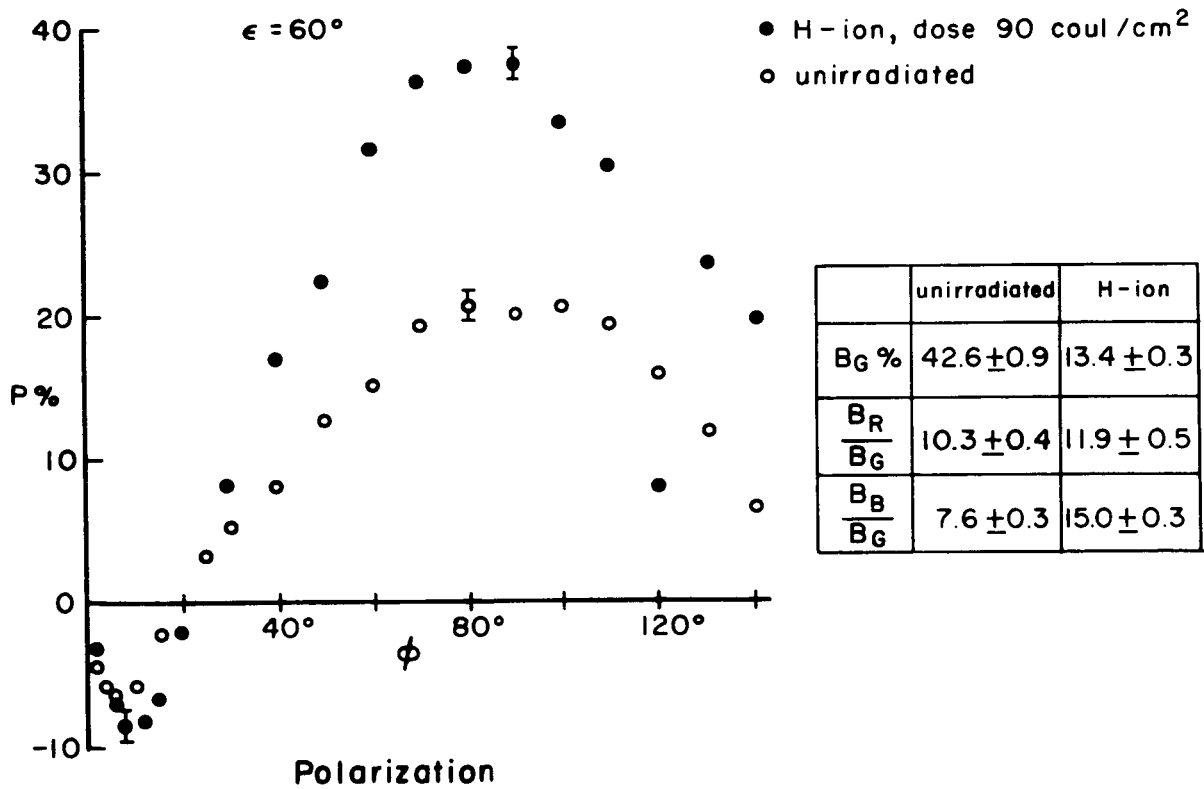
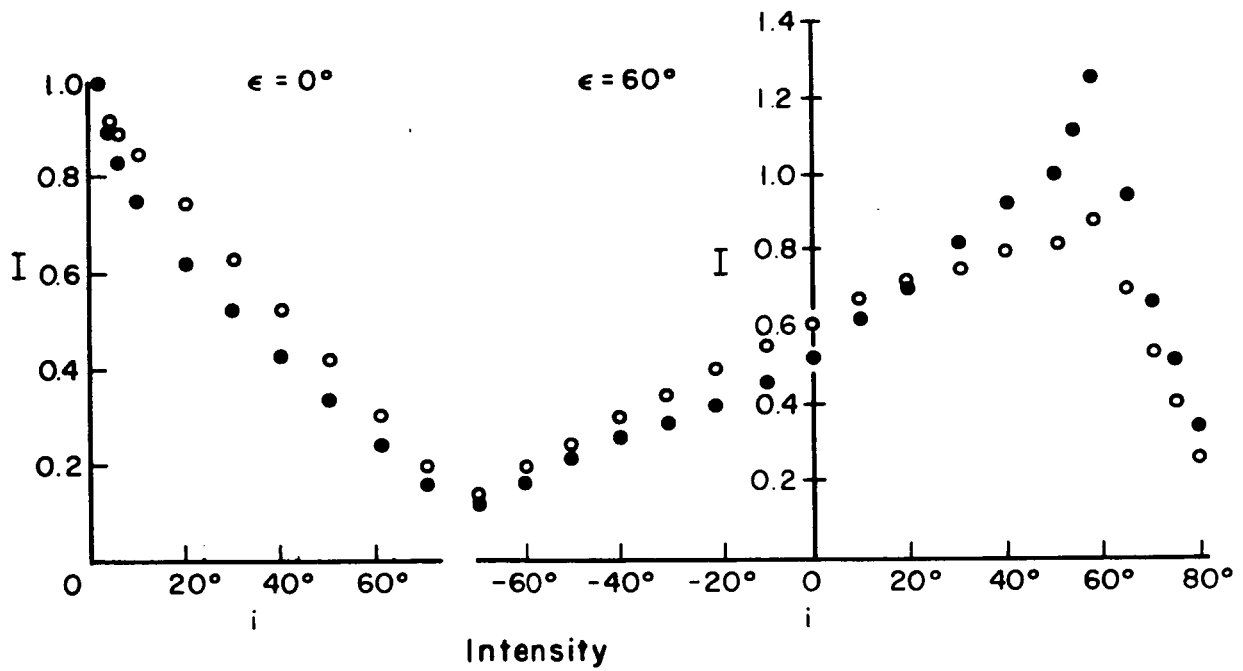


FIGURE 18. Mepherine synite (Particle size < 10 $\mu$ ).

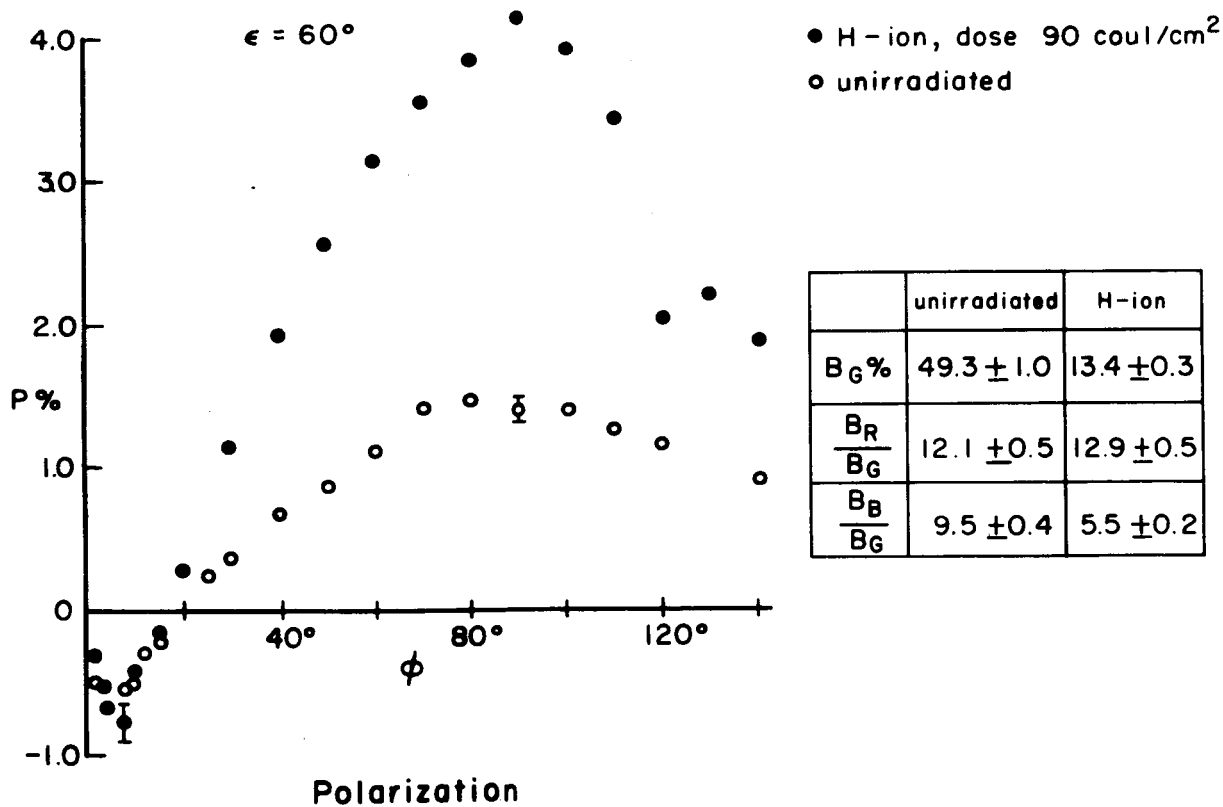
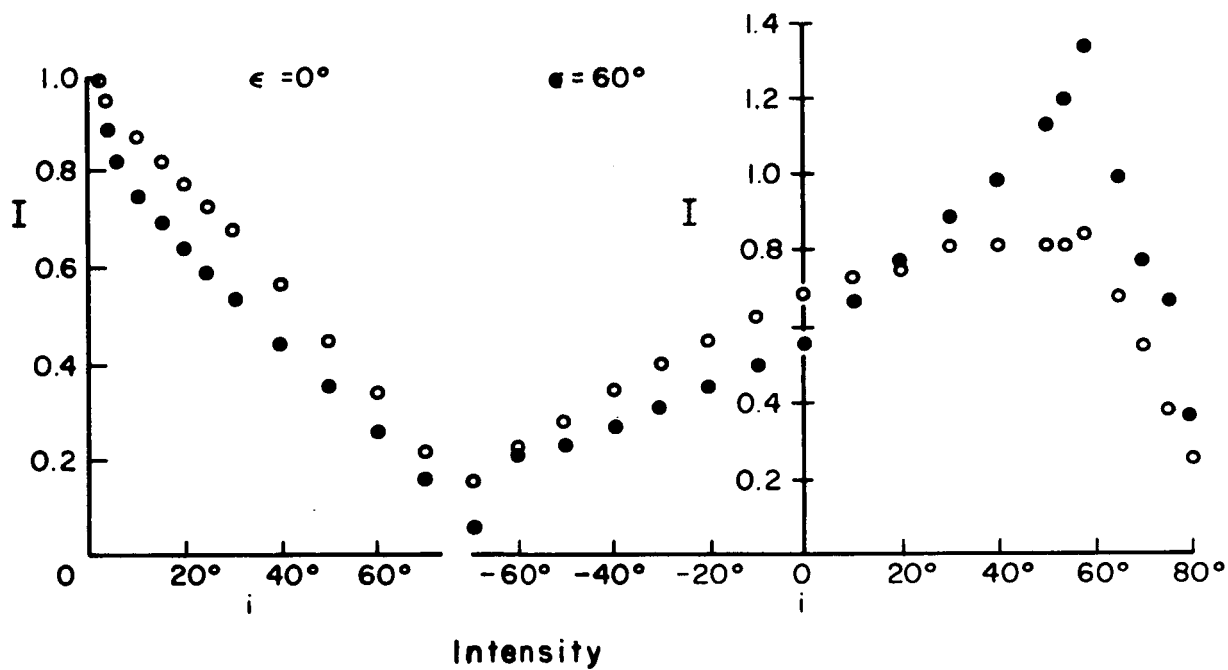


FIGURE 19. Rhyolite (Particle size  $< 10\mu$ ).

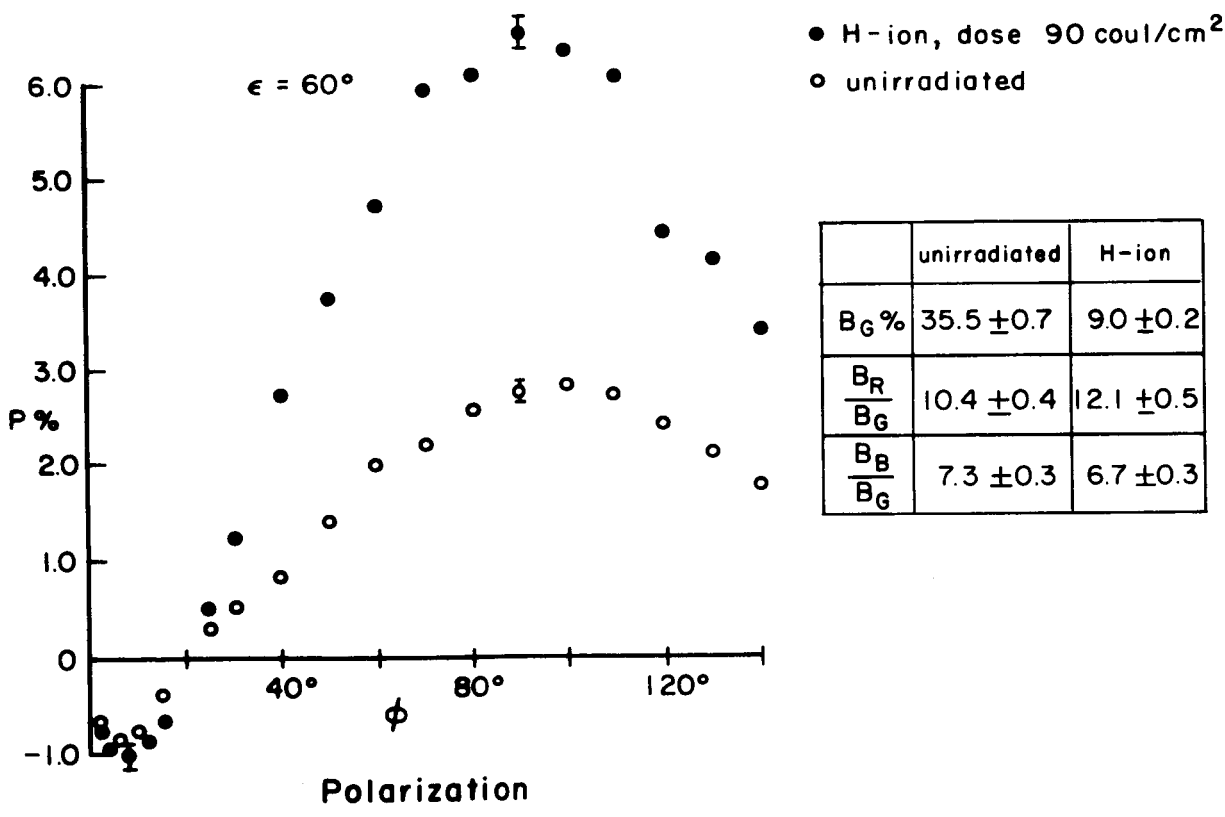
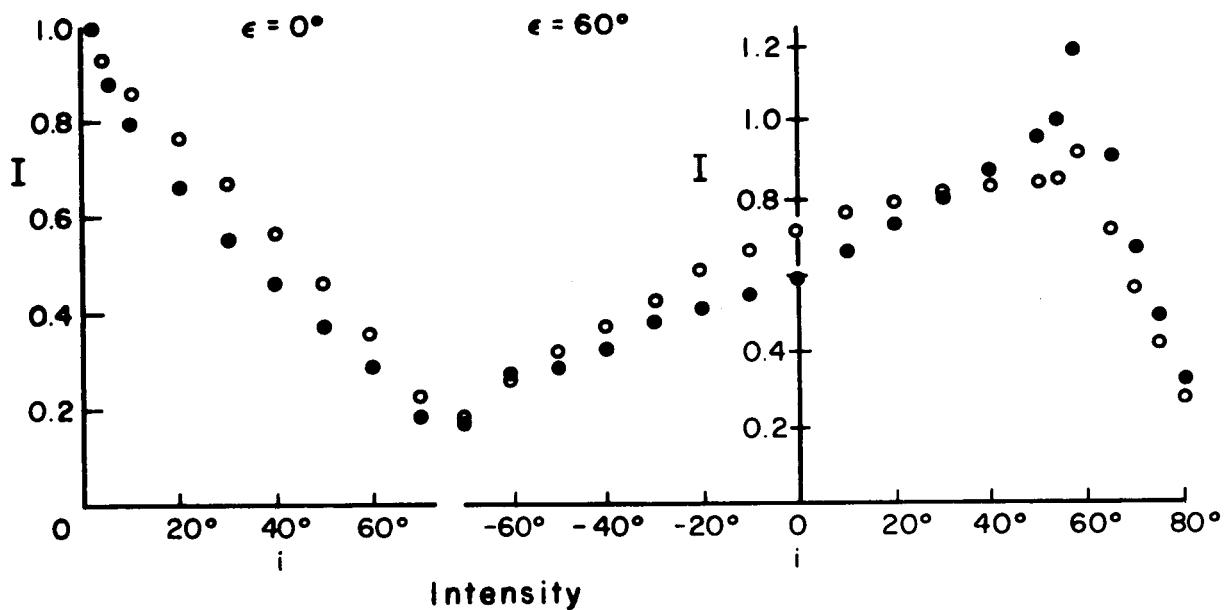


FIGURE 20. Olivine basalt porphyry (particle size < 10 $\mu$ ).

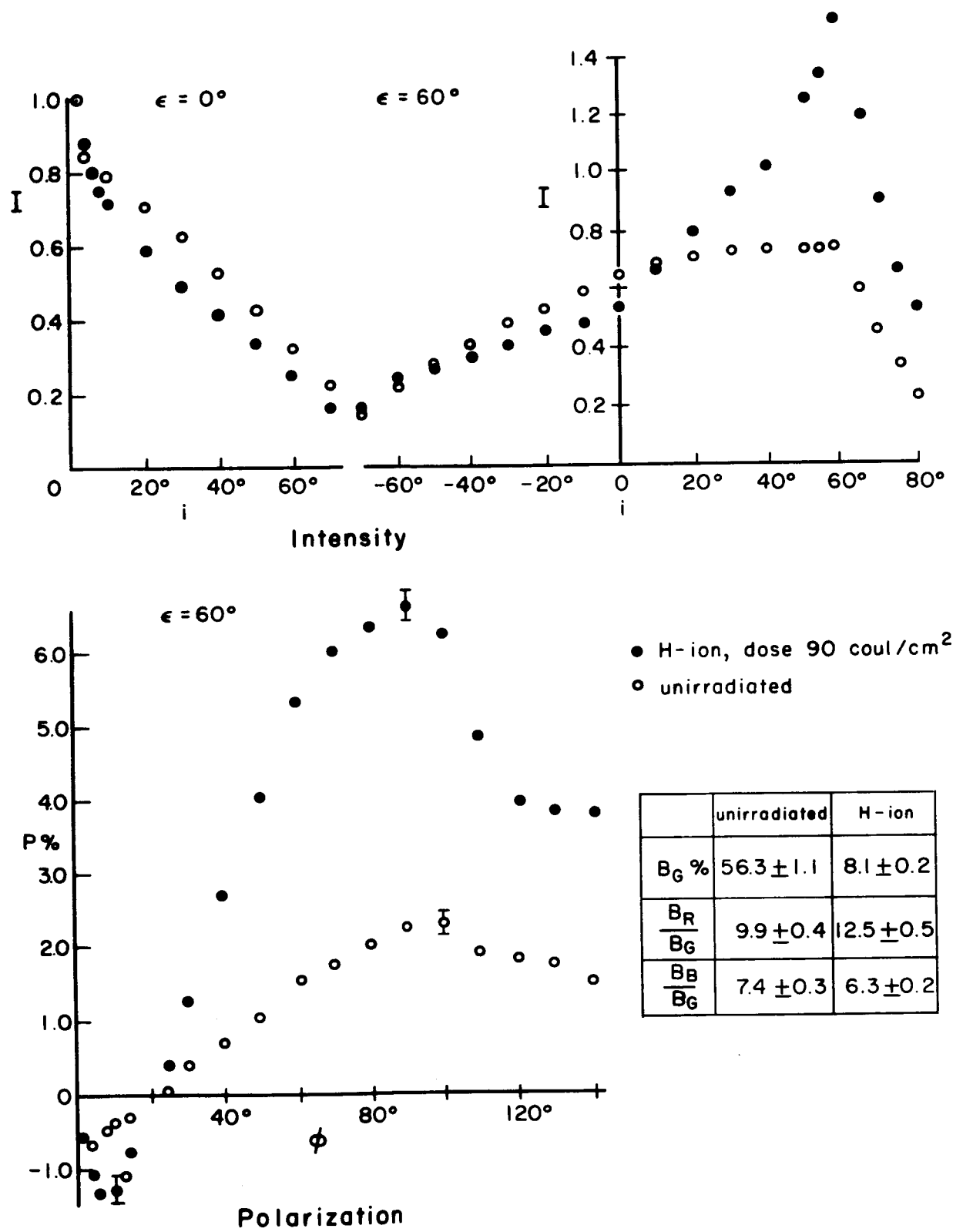


FIGURE 21. Dunite (particle size  $< 10\mu$ ).



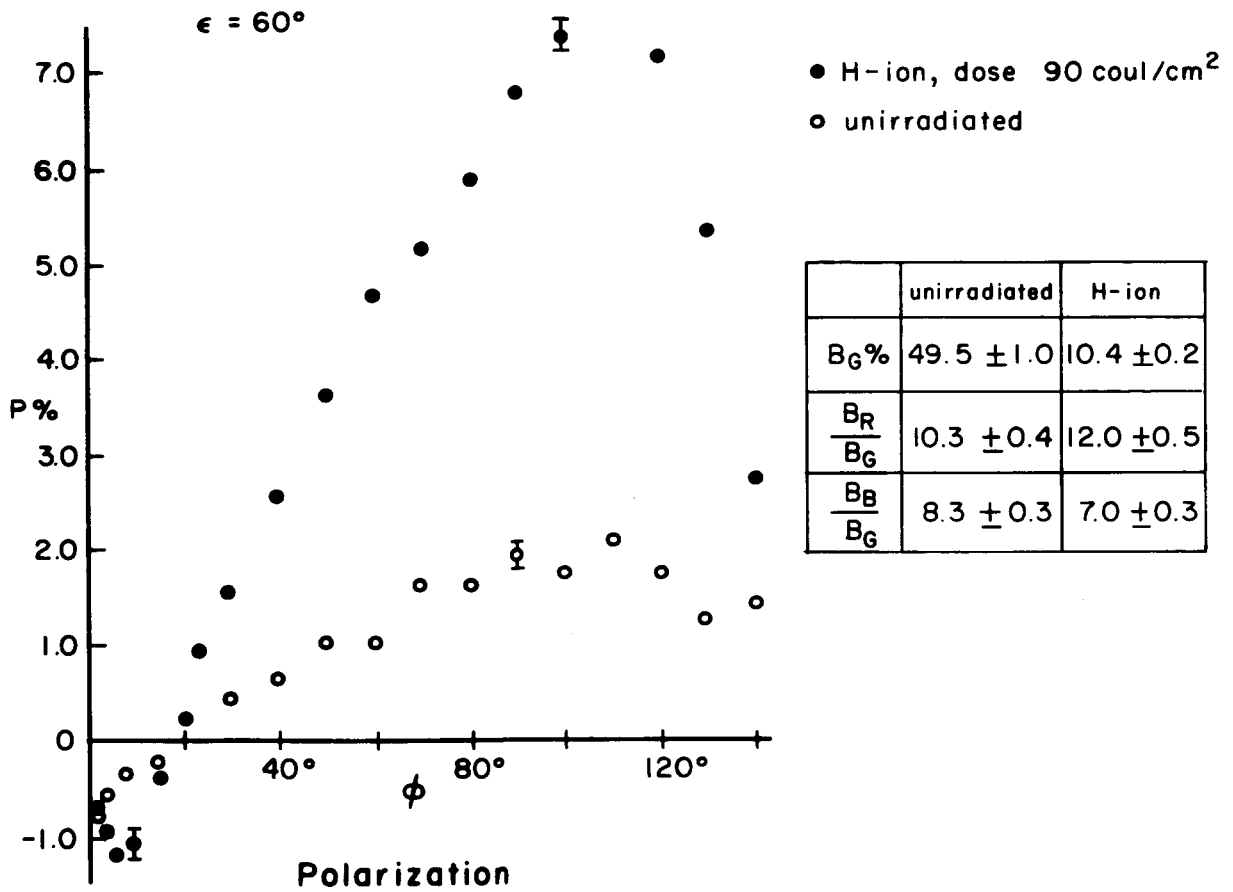
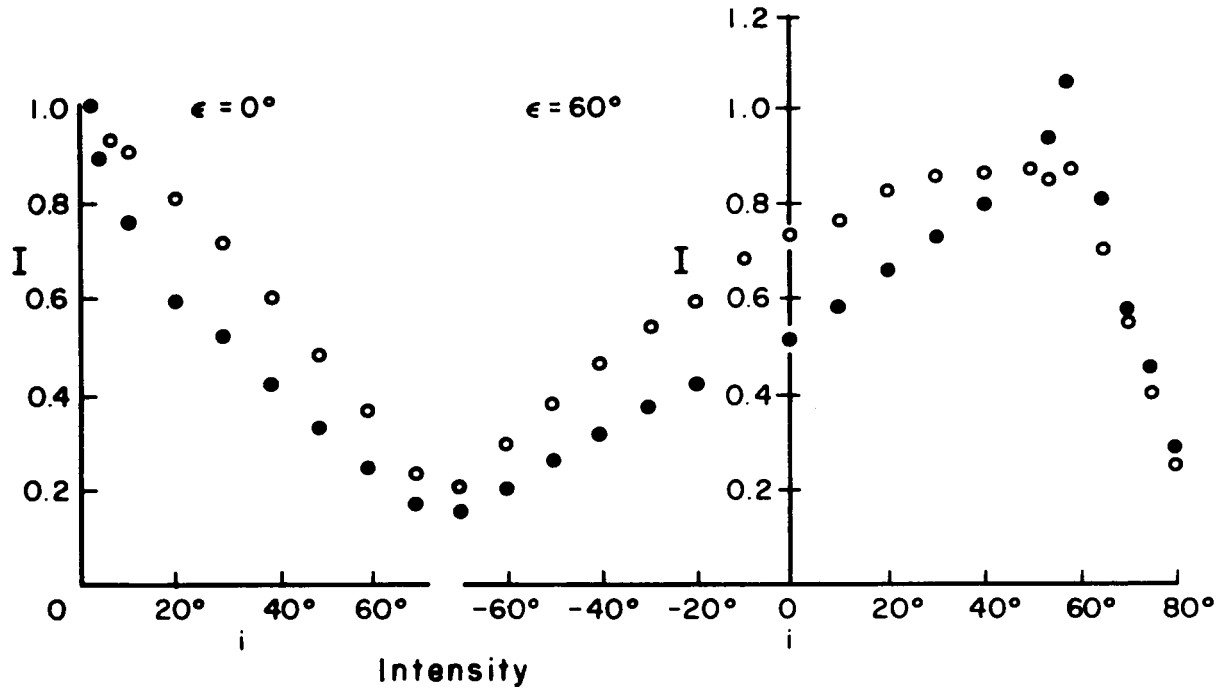


FIGURE 22. Tektite (particle size  $< 10\mu$ ).

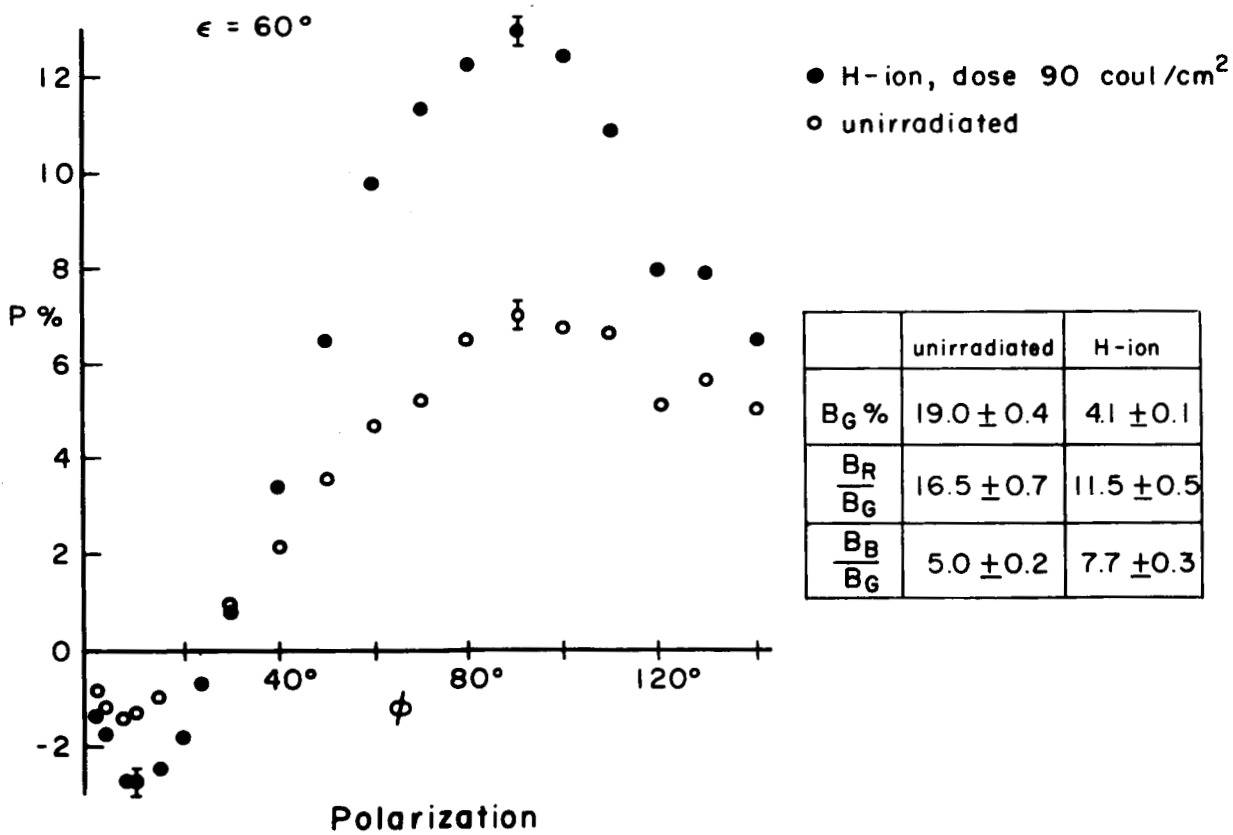
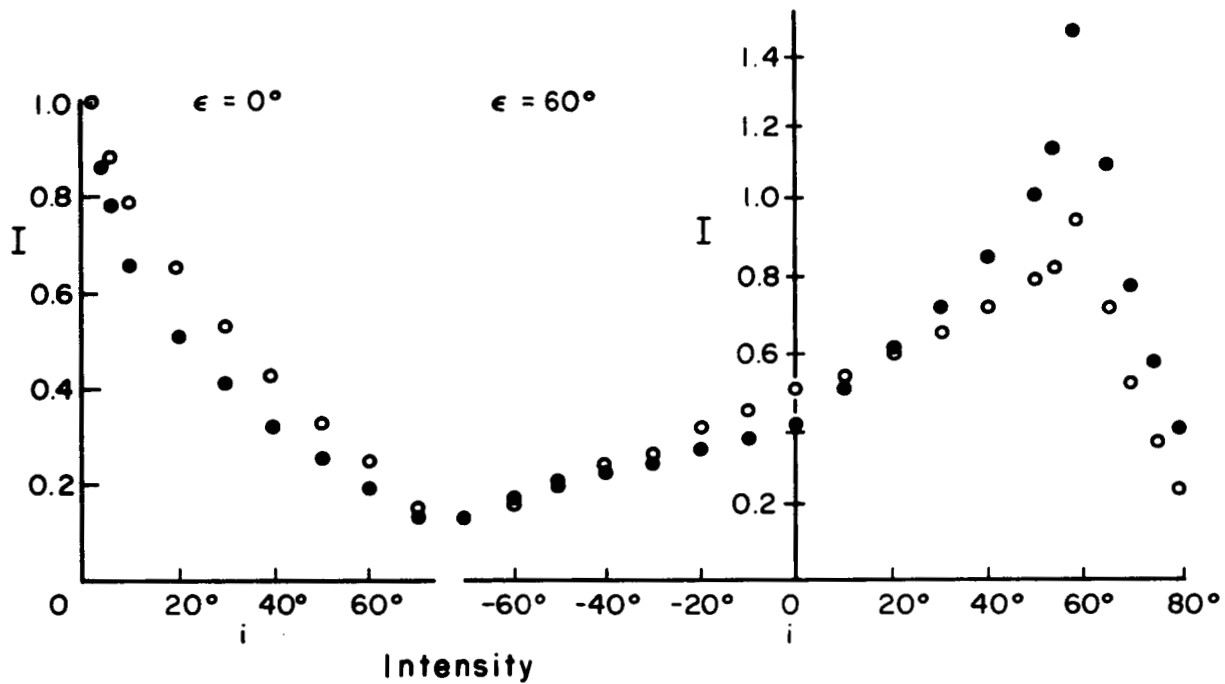


FIGURE 23. Volcanic ash (particle size  $< 10\mu$ ).